Nanoparticle Delivery of siRNA

Multi-functional Upconverting $NaYF_4$ Nanoparticle siRNA Delivery System for Knockdown of SOD1, a Gene Linked to ALS

A Major Qualifying Project Report Submitted to the Faculty

of

Worcester Polytechnic Institute

in partial fulfillment of the requirements

for the Degree of Bachelor of Science

Steven Buchholz and Sam Kesseli

March 3, 2012

Principal Investigator:
Dr. Gang Han

Advisors:
Dr. Marsha Rolle
Dr. Robert Dempski

Contents

Authorship

Both authors contributed to Chapters 1, 2, 3, 4 and 8.

Sam authored Chapters 5 and 7.

Steve authored Chapter 6.

Both authors contributed to the editing and formatting of the final report.

Acknowledgements

We would like to extend our thanks to the following individuals for their continued assistance, guidance, and advice throughout the completion of this Major Qualifying Project:

Dr. Gang Han of UMass Medical School, for his support in coordinating and sponsoring our research

Dr. Marsha Rolle of Worcester Polytechnic Institute, for her guidance, advice, and encouragement throughout the entirety of the project

Dr. Robert Dempski of Worcester Polytechnic Institute, for his support and advice

Dr. Siobhan Craige for her generous advice and assistance with the western blotting protocol

Jie Shen and Yukei Zou of UMass Medical School, for their support and assistance throughout our research

Lisa Wall of the WPI Biomedical Engineering department for her assistance in ordering supplies

Table of Figures

Table of Tables

Abstract

Upconverting nanoparticles (UCNP) were characterized for their properties as siRNA transfection agents, in an approach to target superoxide dismutase 1 (SOD1), a protein implicated in all forms of amyotrophic lateral sclerosis. In this study, two UCNP designs were considered and tested: (1) $NaYF_4$:Yb,Er@$NaYF_4$ core/shell nanoparticles with polyethylene imine (PEI) coating and (2) $NaYF_4$:Yb,Er@CaF_2 core/shell nanoparticles with a citric acid/PEI coating. The $NaYF_4$-shell particles exhibited a working range less than 20 µg/mL to maintain 80% cell viability in HeLa cells. Additionally, these particles exhibited effective plasmid and siRNA delivery, quantified through green fluorescent protein (GFP) expression and SOD1 knockdown in Western blots respectively. The CaF_2–shell particles had a greater working range, up to 50 µg/mL at 80% cell viability, but did not demonstrate effective plasmid or siRNA delivery. Continued research will be required to optimize a UCNP design which combines high cell tolerance with efficient payload delivery.

Chapter 1: Introduction

Amyotrophic Lateral Sclerosis (ALS) is a neurodegenerative disease characterized by degeneration of afferent neurons in the motor cortex, brainstem, and spinal cord. ALS is progressive and fatal; patients present with symptoms of muscle weakness and paralysis. The disease is fatal 3 to 5 years after diagnosis (Mitchell, 2007). No effective treatment exists for ALS patients, presenting a great need for an innovative therapy.

Recent research has focused significant effort on one protein in particular, superoxide dismutase 1 (SOD1), because it is the most common factor associated with ALS (Grad, 2011). Mutated forms of SOD1 have been genetically linked to 20% of fALS cases, (Rosen, 1993) and misfolded SOD1 has been found in the spinal cords of all ALS patients; implicating SOD1 universally in the disease. (Forsberg, 2010)

Small interfering RNA can be developed to specifically target messenger RNA, in order to silence target proteins. In the case of ALS, silencing mutant or misfolded SOD1 may halt the progression of the disease. This potential offers an alternative approach to ALS treatment, but would require the introduction of siRNA molecules into the afferent motor neurons. Current siRNA delivery methods are not suitable for this application, mainly due to toxicity (Luo, 2000).

Upconverting nanoparticles (UCNPs) represent a novel platform for siRNA delivery that may contribute additional functionalities during treatment. These may include tissue imaging, particle tracking, cell targeting, and cell penetration. If UCNPs could be optimized for siRNA delivery, they may provide the first effective foundation for ALS treatment.

In subsequent chapters this project will elaborate on the potential utility of UCNPs for siRNA delivery, our project strategy, alternative designs, and design verification. Furthermore, experimental results will be described and discussed to validate UCNP designs for siRNA delivery. From these, conclusions will be drawn and recommendations made for future studies.

Chapter 2: Literature Review

Amyotrophic Lateral Sclerosis

Amyotrophic Lateral Sclerosis (ALS) is a neurodegenerative disease characterized by degeneration of the afferent neurons in the motor cortex, brainstem, and spinal cord. ALS is progressive and fatal; patients present with symptoms of muscle weakness, paralysis, dysarthria and dysphagia (difficulty speaking and swallowing, respectively), and ultimately respiratory compromise. The degeneration of the corticospinal motor tract causes the denervation in muscle fibers that induces this fatal muscle atrophy (Mitchell, 2007). Other names for ALS include Motor Neuron Disease, Charcot's Disease, and, Lou Gehrig's Disease.

ALS can manifest in two ways; either as the limb-onset or the bulbar-onset form of the disease. In limb-onset ALS, the primary symptoms are first seen in the arms and legs; whereas with bulbar-onset, the disease first affects the muscles associated with speaking and swallowing. Patients develop symptoms of both forms as the disease progresses, although ordinarily one form takes precedence. For about two thirds of patients, initial symptoms indicate limb-onset ALS. Survival after diagnosis for the limb-onset form is an estimated 3 to 5 years and for bulbar-onset patients, survival is typically 2 to 3 years. (Wijesekera, 2009)

Further characterization of ALS can be made based on its origin; either sporadic (sALS) or familial (fALS). Sporadic ALS refers to the seemingly random development of the disease, as the risk factors are not clearly identified. Familial ALS is genetically induced, and can be inherited. The average annual incidence of ALS between Europe and North America is reported as 1.89 per 100,000 (Worms, 2001). In the United Sates, there are an estimated 5,000 new diagnoses each year (NINDS, 2011). Of these cases, 5-10% are familial (fALS) by autosomal dominant inheritance, and an estimated 20% of fALS cases are directly linked to a mutation in the Superoxide-Dismutase 1 (SOD1) gene (Wijesekera, 2009).

Etiology

The etiology and risk factors that induce ALS are not yet identified, though many potential pathways to the disease have been identified. Two major, interrelated mechanisms that contribute towards ALS are glutamate excitotoxicity and oxidative stress.

Oxidative stress damages proteins, lipids, and DNA within the cell. The formation of superoxide radicals (O_2^-) within the cell occurs naturally; most frequently at the mitochondria where electrons in the electron transport chain 'leak' onto molecular oxygen. The cell has natural anti-oxidant mechanisms to reduce these potentially harmful radicals, notably the SOD1 enzyme. However, without functional superoxide scavenging, reactive oxygen species can accumulate, resulting in the aforementioned cellular damage. Figures 1 and 2 demonstrate the role of normal SOD1 in a neuron (Figure 1), and the consequences of mutant SOD1 (Figure 2). One specific reactive oxygen species, peroxynitrite ($ONOO^-$), forms in a reaction between superoxide and nitric oxide (NO^-). Post-mortem studies have identified peroxynitrite-mediated oxidative damage in both sporadic and familial ALS patients, linking oxidative stress directly to ALS (Barber, 2006).

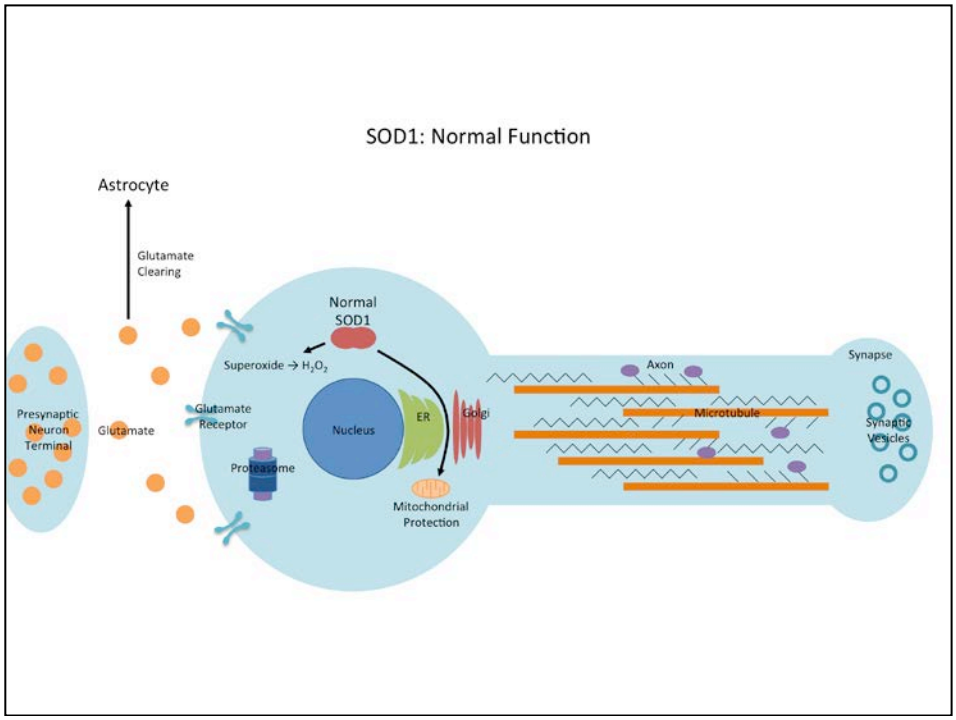

Figure 1: Normal SOD1 function in neuron

Another study also suggested oxidative stress played a role in the inactivation of glutamate transporters (Trotti, 1999). Glutamate serves as an excitatory neurotransmitter in the central nervous system (CNS) and its neurotransmission is mediated by receptors in the synaptic cleft. Excess accumulation of glutamate in the cleft can induce excitotoxicity; the over-activation of neurons resulting in cell death. This excitotoxic mechanism has been implicated in ALS, as well as other neurodegenerative disorders such as Alzheimer's and Huntington's disease. Many studies have focused on the Excitatory Amino Acid Transporter (EAAT) 2, for its major role in glutamate removal. One study utilized ALS mouse models to compare grip strength with ALS mice that over expressed EAAT2, and found that strength was significantly prolonged. However, neither lifespan nor paralysis onset were improved, suggesting that glutamate excitotoxicity contributes to ALS but is not the underlying cause. (Guo, 2003)

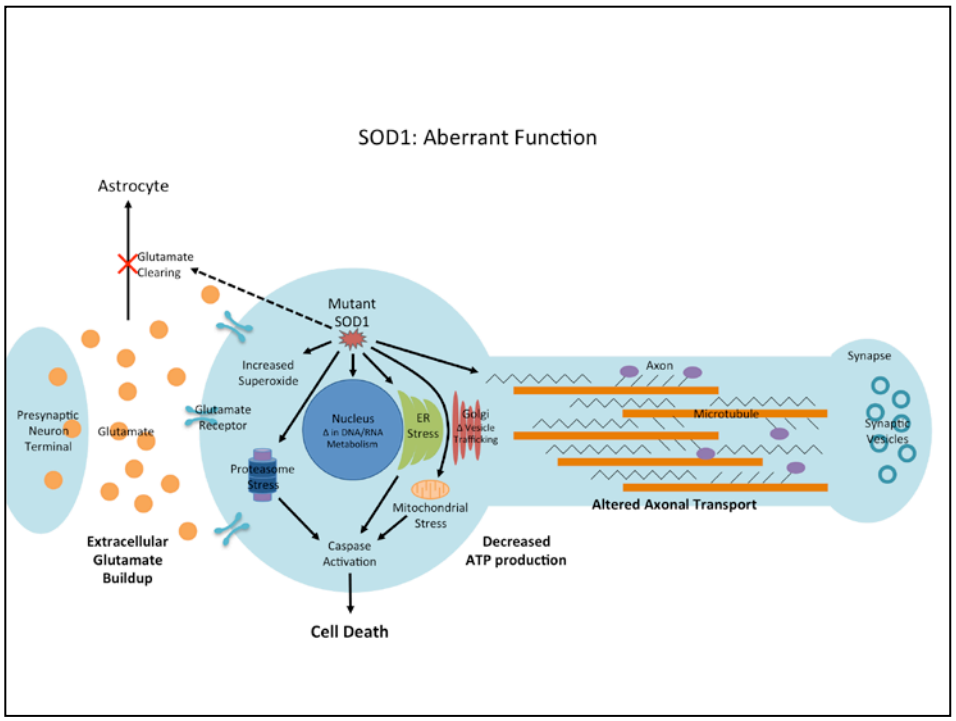

Figure 2: Consequences of mutant SOD1 in neuron

The interrelation between these pathways demonstrates the complex, multifactorial etiology associated with ALS. Additional mechanisms have been proposed and studied such as calcium-dependent mitochondrial dysfunction (Jaiswal, 2009), protein

aggregation (Mitsunori, 2001), and deficient neurofilament-mediated axonal transport (Williamson, 1999), and in each of these studies, mutant SOD1 was implicated.

Superoxide Dismutase 1

Cu, Zn-superoxide dismutase (SOD1) is a superoxide scavenger found in the cytoplasm of most human cells. Normally, it is part of the family of oxidoreductases acting on superoxide radicals as the acceptor (Enzyme Classification Number: EC 1.15.1.1). Disproportionation, also called dismutation, is the simultaneous oxidation and reduction of reagents. (IUPAC, 1997) Oxygen free radicals are a natural intermediate of intracellular chemistry. A constant low-level concentration of these species is maintained in the cytosol through the work of anti-oxidants and free-radical scavenging enzymes such as SOD1. (Shaw, 1997)

Aberrant SOD1 is the most common factor associated with ALS. (Grad, 2011) Mutated forms of SOD1 have been genetically linked to 20% of fALS cases. (Rosen, 1993) Novel antibodies have revealed misfolded SOD1 in the spinal cords of both fALS and sALS patients; implicating SOD1 universally in both forms of the disease. (Forsberg, 2010) In the case of fALS, both missense and nonsense mutations have been associated with SOD1 misfolding leading to disease pathology. (Pasinelli & Brown, 2006) In sALS, the cause of SOD1 misfolding is still unknown. However, recent studies have shown that oxidized forms of SOD1 and mutant forms share an aberrant conformation pointing to a potential pathology. (Bosco, 2010)

Whether in the mutated form or in the misfolded form, SOD1 toxicity is twofold. Toxicity is primarily attributed to a loss of specificity in the binding pocket, which leads to aberrant redox chemistry. (Pasinelli & Brown, 2006) Toxicity is also attributed to the mis-localization of the toxic enzyme. The toxic enzyme is moved to different organelles within the cell and secreted outside of the cell. This toxicity is multi-factorial as the SOD1 mis-localization within the cell, specifically within motor neurons, adversely affects a number of different processes including: DNA and RNA metabolism; vesicle trafficking in the Golgi apparatus; ATP production and calcium buffering in the mitochondria; axonal transport and neurofilaments; and proteasomes. Stress on the

proteasomes, mitochondria, and endoplasmic reticulum (ER) signals caspase activation and apoptotic pathways ultimately bringing about neuronal death. (Pasinelli & Brown, 2006) SOD1 mis-localization outside of the neurons due to monomerization of misfolded proteins causes protein aggregation outside of the cell. These protein aggregates can undergo macropinocytosis and induce misfolding of native SOD1, thereby propagating the toxic effects along the spinal column. This is a potential cause of the progressive nature of ALS. (Grad, 2011) The ubiquitous implication of SOD1 across all forms of ALS suggests that it may be a universal and effective target for development of treatment.

Current ALS Treatments

Only one drug, Riluzole, has been approved by the FDA for treatment of ALS, although other experimental drugs are currently in phase II and III trials. The therapeutic efficacy of these drugs is uncertain and improvements in survival are marginal at best, justifying the need for novel and innovative new therapies.

Riluzole, 2-amino-6-(trifluoromethoxy)benzothiazole, is hypothesized to inhibit glutamate transmission, offering the potential to minimize toxic, post-synaptic glutamate accumulation. Though the mechanism of action is unknown, Riluzole was found to be safe at doses of 200mg in phase I clinical trials. A double-blinded, placebo-controlled study conducted in 1994 examined 155 patients with both limb-onset and bulbar-onset ALS. After one year, patients whom received Riluzole had a median survival rate only 83 days longer than patients in the placebo group (532 vs. 449 days). (Bensimon et al., 1994)

Currently in phase III trials, Ceftriaxone has been publicized by the ALS Association as another potential drug for ALS therapy. Ceftriaxone is an antibiotic of the β-Lactam antibiotic family; these antibiotics are known to induce expression of EAAT2, the main glutamate transporter in glial cells of the central nervous system (Miller, 2005). If successful, this approach would minimize post-synaptic glutamate accumulation and prevent excitotoxicity-induced neuron death. Currently, the US National Institutes of Health that are conducting the trial have not published any results.

Dexpramipexole is another drug currently in phase III clinical trials, though no results have been published. In phase I and II trials, dexpramipexole was safe at doses of 150 mg twice daily (Biogen Idec, 2011). It is the R enantiomer of pramipexole, a dopamine agonist used to treat Parkinson's Disease. The R enantiomer, dexpramipexole, has no dopaminergic effects but is hypothesized to improve mitochondrial function and treatment has resulted in prolonged survival in ALS mice (Zinman, 2011).

Thus, for patients with ALS, there is a need for an alternative therapy. The only FDA approved drug, Riluzole, marginally increases lifespan, though no therapy exists to improve the quality of life or slow the progression of the disease. The identification and limited understanding of SOD1's role in ALS presents an opportunity to treat what may be the major underlying cause of the disease. Until now, treatments have targeted downstream effects of aberrant SOD1 function; by disrupting the expression of genes encoding SOD1, disease progression could potentially be halted. The application of RNA interference may allow for knockdown of mutant SOD1 gene expression, and thus a new approach in ALS therapy.

RNA Interference

Since the discovery of endogenous cellular pathways of messenger RNA regulation in plants and the elucidation of double-stranded RNA interference (RNAi), the potential of microRNAs (miRNAs) for therapeutic application has been widely studied. The efficacy of RNAi as a therapy has been extensively documented in laboratory animals, but has not gone beyond phase I clinical trials in humans (Grimm, 2007). The basic mechanism can be broken down into two pathways each beginning with small hairpin RNA (shRNA). The miRNA is produced either endogenously in the nucleus, or exogenously and delivered into the cell by artificial means. Endogenous miRNA goes through a two-stage modification prior to exiting the nucleus including RNA polymerase II or III and the Drosha complex. Exogenous, or synthetic, miRNA is designed to mimic this mature form, shRNA (Paddison, 2008).

Once in the cytoplasm, the shRNA, or double-stranded RNA (dsRNA), is acted upon by Dicer, an enzyme which cleaves off its loop structures producing a small

interfering RNA (siRNA). siRNA signals the inhibition, degradation, or cleavage of a specific mRNA. This target mRNA is determined by complementation with one of the two strands of the siRNA, which allows incredible specificity in targeting a specific mRNA sequence using this mechanism. This activity is carried out when the siRNA complexes with the RNA-induced silencing complex (RISC). It is the RISC that actually carries out the activity involved with RNA interference but it is the siRNA sequence that determines the target (Paddison, 2008).

Based on this system, siRNA can be developed using complementary base pairing with a target mRNA. This treatment is specific to the point that it can even target mutant versus wild-type strands of mRNA and thus correct autosomal dominant strains of genetically-based diseases by knocking down the mutant-type mRNA and allowing the wild-type to be expressed. One remaining challenge is the development of a mechanism to deliver siRNA into target cells.

Current siRNA Delivery Vectors

In the past thirteen years, four primary methods of siRNA delivery have been developed: (1) viral vectors, (2) electroporation, (3) chemical modification, and (4) transfection. (Chen, 2010) Each method has its own benefits and limitations. These need to be explored in order to decide upon the method best suited to neuronal delivery.

Viral vectors have been used extensively in biotechnological applications for the introduction of RNA- and DNA-based exogenous materials (Luo, 2000). For siRNA delivery systems, the best-suited vectors are retroviruses, adeno-associated viruses, and lentiviruses. (Shi, 2003) The benefits of viral vectors are high efficiency and reproducibility, effective delivery into primary and non-dividing cells, and stable expression *in vivo*. The limitations of this vector include immunogenic response of the host organism, mutagenic properties of the host virus, and generation and titration of virus particles. (Chen, 2010) Recent studies have shown that retrograde transport of viral vectors through the motor neurons via muscular injection did not transport the therapy into the central nervous system. (Towne, 2011)

Electroporation is a technique developed *in vitro* that has only recently been studied for *in vivo* applications. Electroporation utilizes a voltage pulse applied across the membranes of the target cells to open up pores in the membrane that will allow the entry of siRNA molecules. The benefits of electroporation are that it is noninvasive and it does not induce nonspecific immune responses. The limitations are that pulse conditions need to be optimized based on tissue density and depth, and that the cells near the sites of pulse application can be damaged by the electrical current. (Chen, 2010)

Chemical modification involves covalently linking specific targeting or protection molecules to the siRNA itself to allow for transport into cells. This is achieved either through the modification of specific bases at the ends of the siRNA or the addition of lipids to the 3' end of the siRNA. The benefit of this vector is that the modified siRNA exhibits improved resistance to nuclease degradation compared to unmodified siRNA. However, two major limitations are the reduction in the activity of the modified siRNA and the production of toxic chemicals (Luo, 2000) upon the degradation of a modified siRNA molecule. More research is still being done to optimize this delivery vector. (Chen, 2010)

Transfection is the use of lipids, polymers, or other conjugates to encapsulate and deliver siRNA (Luo, 2000). The siRNA is typically encapsulated in a micelle or other similar structure and then brought into the cell through clathrin-mediated endocytosis. The benefits of using transfection agents are their high efficiency and reproducibility and their ease of use in most cell types. The limitations are that they can lack cell specificity, lipid-based approaches tend to disrupt function of the cell membrane while other approaches can invoke an immune response, and the size of the particles are hard to control. One commercially available lipid-based transfection agent, Lipofectamine™ 2000, has demonstrated excellent transfection efficiency, although it is also cytotoxic (Clements, 2007).

Combining the technologies of chemical modification and transfection with the newer field of nanotechnology has led to a novel approach that safely and effectively delivers siRNA while introducing other functionalities. The entrance of nano-scale

therapeutics into pharmaceuticals began with the development of biologically active polymers. (Duncan, 2003) Polymers such as polyethylene glycol (PEG) form the basis for polymer-treatment conjugates. The polymer acts as a vessel to transport and protect the therapeutic molecule of interest. Once these conjugates were scaled down to the single molecule level, nano-scale therapeutics was born. Polymer chemistry allowed for the formation of targeting structures, polymeric drugs, polymer-protein conjugates, polymer-DNA complexes, and polymeric micelles. (Duncan, 2003) This was joined by inorganic nanoparticles based on heavy metal and metalloid chemistry, typically gold or silver and silicon, used for their unique optical properties and biocompatibility. (Hirsch, 2003) More recently, attempts have been made to combine these two approaches by using a core-shell particle of inorganic material surrounded by a surface coating of polymeric and/or biological molecules resulting in multifunctional nanoparticles (NPs). (Ferrari, 2005) The organic surface coating creates an affinity for biological molecules. This can be used similar to transfection for transporting nucleic acids, i.e. siRNA, into target cells.

Nanoparticles as Transfection Agents

Multifunctional nanoparticles (NPs) make it possible to combine cell targeting molecules, surface-interface lipids, treatment molecules, and optical activity into a single platform. (Serda, 2011) By conjugating the active molecules to the surface of the inorganic particle, NPs have the potential to overcome the common limitations associated with other transfection methods, specifically immune response and membrane disruption (Massich, 2009). However, NPs do present their own challenges.

A primary challenge is targeted and controlled release of the therapeutic molecule. Depending on payload interaction, typically electrostatic stacking interactions or covalent linkage, the NP will demonstrate different release profiles. With electrostatically coupled molecules, the release is dependent upon diffusion within the surrounding environment. Once the particle enters an environment that is more electrostatically favorable, the payload is released. With covalent linkage, the release is steadier; as the particle coating interacts with degradative enzymes, the payload is slowly released from the surface. (Duncan, 2003)

Controlled release is achievable through controlled surface chemistry or external triggers. (Ferrari, 2005) By studying the electrostatic environment into which release is desired, NP surfaces can be tailored to the target. The difficulty becomes that this surface may not be the most favorable for interacting with the payload, so release must be balanced with dosage. With covalent linkage, it is possible to use electromagnetic radiation (EMR) to release the treatment molecules once the particle has reached the desired location (Serda, 2011). Resonance frequencies are used to excite the bond attaching the treatment molecule to the particle. Once the proper wavelength and frequency are determined, external EMR is used to stimulate the bond until release is achieved. This is typically achieved with lasers. The difficulty with this method is ensuring that the external signal is strong enough to release the treatment and yet weak enough to not damage native molecules. (Serda, 2011)

One secondary challenge is tracking NPs once they have been introduced into a tissue culture or organism. A simple solution is to tag the surface with fluorescent molecules. There are two major types of fluorescing molecules, endogenous and exogenous fluorophores. (Lakowicz, 2006) Both of these types of molecules typically need an external stimulus for activation. An incoming photon excites the electrons of the fluorophore causing it to jump to a higher energy state. As the electron loses energy, it moves back to a lower energy state and emits a photon with equal or lower energy than the original. (McQuarrie, 1997) This means that molecules that emit photons in the visible range will need to be stimulated in the visible (400-740 nm) or ultraviolet (UV,1-400 nm) spectra, a range that can be disruptive to biological molecules. Additionally, biological tissues typically absorb in the visible and UV spectrum making penetrance difficult for larger cross sections of tissue. (Lakowicz, 2006) For exogenous fluorophores such as cyanine dyes, conjugation to the surface usually inactivates the fluorescence and so the molecule must be released from the surface before detection. (Congdon, 2010)

Upconverting Nanoparticles (UCNPs)

Upconverting Nanoparticles (UCNPs) are core/shell nanoparticles that incorporate lanthanide metals to provide fluorescent properties. Lanthanide metals absorb in the infrared (IR) range (0.74-300 μm) and fluoresce in the IR, visible, and UV ranges.

Coupling specific metals within the UCNP core yields an upconversion of the incoming photon. This enables the potential to use low energy lasers in the IR range, that will not affect the tissue surrounding the particle, to the release molecules coupled to the particle itself (Han, 2009) This also provides a method of tracking the particle as it moves through the organism. Biological tissues typically absorb in the visible and UV spectra. Since Lanthanide metals can fluoresce in the IR range, the signal will not decay as it passes through the tissue.

The core consists of a base of sodium yttrium (III) fluoride ($NaYF_4$) ceramic that is doped with various concentrations of ytterbium (Yb) and either erbium (Er) or thulium (Tm). The Yb acts as a photon acceptor excited at 980 nm. It then passes the energy to either Er or Tm. As more energy is passed to Er or Tm, the electrons are pushed to higher energy states and photons are emitted anywhere in the range of 900-400 nm, which is controlled by the doping ratios of Yb to Er or Tm. This core is surrounded by an electropositive, fluorescently inert shell. The positive shell is used for conjugation of organic materials, such as lipids, proteins, or polymers. It is this outer coating that interacts with biological surfaces and other molecules of interest.

The design team proposed to utilize UCNPs as siRNA delivery vectors for the targeted knockdown of SOD1. UCNPs were assessed for their utility as transfection agents. The cytotoxicity and transfection efficiency associated with UCNPs were characterized in vitro. HeLa human cervical cancer cells were used to conduct these characterizations through a variety of standard biochemical assays.

Chapter 3: Project Strategy

Initial Client Statement and Objectives

Given the potential of siRNA therapies for the treatment of ALS, and the platform of UCNPs as transfection agents, the team developed an initial client statement:

To develop a siRNA delivery system that is safe and effective based on the platform of upconverting nanoparticles for treatment of ALS.

Before the team could put forward a design, several steps had to be taken. First, the stakeholders had to be identified. These stakeholders would then define the objectives and constraints of the delivery system. These criteria are essential to the construction of a design space that meets the requirements of all parties involved while providing flexibility for the team to explore all possible solutions to the problem presented.

The stakeholders were broken down into three primary groups: users, clients, and designers. The users are defined as any persons utilizing the delivery system for the knockdown of target proteins. The short-term users include graduate students and the principal investigator, Dr. Gang Han, while the long-term users include medical doctors, nurses, and patients. The users were considered the main stakeholders in this process. The clients included Dr. Gang Han and his research team, and the design team (Steven Buchholz and Sam Kesseli).

Each stakeholder group contributed different objectives to the design. The users desired a safe and efficacious design that is easy to use and cost-effective. The clients desired a design that would be specific and scalable for continuing the project into animal models. From these, the design team further defined sub-objectives to better measure the outcomes of the design and to ensure that the design criteria were met (See Appendix A: Objectives Tree). These were then discussed with the users and clients to rank the importance of each of the objectives and sub-objectives.

Through pairwise comparison, the relative priority of each objective was determined. The Pairwise Comparison Chart (PCC) is a valuable tool for determining the

priority of objectives. The calculation is binary, so results only indicate which objective is more or less important; it does not gauge *how much* more or less important the objectives are relative to one another. The PCC for the primary objectives indicates that "specificity" is the highest priority, while "efficacy" is of lowest priority. See Table 1 below for the PCC analysis. Each primary objective is listed below by priority.

Table 1: PCC for Design Objectives

	Efficacious	Specific	Scalable	Safe	Total
Efficacious	—	0	0.5	0	**0.5**
Specific	1	—	0.5	1	**2.5**
Scalable	0.5	0.5	—	1	**2.0**
Safe	1	0	0	—	**1.0**

1. Specificity was identified as the most important among the objectives. Specificity was defined by two parameters: specific cell penetration (targeting) and specific gene silencing. Of these two, specific gene silencing holds the highest priority. That is, if the target gene of interest (SOD1) is not accurately silenced, the design fails.

2. Scalability is the second-highest ranking objective of the design. The design should be scalable in three aspects (in order of priority): scalable to in vivo studies, to alternate cell lines, and to different dosages. To succeed as a therapy in ALS patients, the design should satisfy these sub-objectives.

3. Safety is third in the ranked objectives. Although all therapies have side effects, the final design must not cause more harm to the patient than the disease itself, and be non-toxic. Additionally, applying the therapy should pose minimal risk to the administrator.

4. Efficacy will only be relevant if the first three objectives are effectively met. If the therapy is minimally effective, but remains safe, scalable, and specific, the design will be considered successful. An efficacious design will be comparable to other delivery methods currently used in laboratory settings, will show broadband cell penetration, and will consistently present a measurable degree of SOD1 knockdown.

Constraints

The design constraints listed below were identified in collaboration between the clients and the design team. These constraints must be met in full to complete the design successfully.

1. Must be less cytotoxic than Lipofectamine™ 2000
2. Must have positive surface charge
3. Must incorporate UCNP's
4. Must deliver siRNA
5. Must be completed by March 2012

Revised Client Statement

"To design, develop, and optimize an siRNA delivery system based on the platform of lanthanide-doped UCNPs that is specific to the target protein and target cells, scalable to in vivo models and multiple cell lines, safe (less cytotoxic that Lipofectamine™ 2000) and efficacious in comparison to standard transfection agents for sequence-specific knockdown of SOD1, a gene linked to fALS. Additional functionalities should include cell targeting and penetration, and siRNA protection from RNase for in vivo siRNA tracking."

Design Approach: Experimentation

To effectively evaluate the preliminary and final designs for a siRNA delivery system, a standardized battery of laboratory tests was performed. The fulfillment of each objective was gauged by the outcome of these tests. Below are descriptions for each of the major experiments performed, and their measurable outcomes. They are described in the order they were performed.

The MTT assay, named for its active reagent, 3-(4,5-Dimethylthiazol-2-yl)-2,5-diphenyltetrazolium bromide, is an *in vitro* assay used to determine cell viability, and will serve as the measure of safety for the design objectives. The test measures the cellular conversion of the tetrazolium salt into a formazan dye product. After four hours incubation time with MTT, a stop solution (SDS diluted in HCL) is added to solubilize the formazan product. The quantity of soluble formazan dye is directly proportional to the quantity of viable cells. In a cell culture plate, the absorbance of solubilized samples can be read at an absorbance of 570nm, thus quantifying the cytotoxic effects of the design and the experimental dose.

Agarose gel electrophoresis enables the determination of the optimal ratio of plasmid DNA to NP for transfection. Nanoparticle/DNA aliquots were loaded into the gel at varying ratios. During electrophoresis, excess, unbound DNA moved down the lanes of the gel. Ethidium Bromide (EtBr) intercalating agent can be used to label the plasmid DNA. Quantification of the band intensity for each lane enabled the design team to determine the ratio where the NPs first bind 100% of the DNA, leaving no measurable unbound DNA in the lanes of the gel.

A spectrofluorometer was used to determine the RNA-Nanoparticle binding ratio. First, RNA is exposed to EtBr (Excitation: 540 nm, Emission: ~590 nm) to determine baseline fluorescence. Nanoparticles were incrementally added, which upon binding with RNA, freed the EtBr. The ratio of particle to RNA concentration was determined when the fluorescence first reached a minimum; at this point the maximum quantity of RNA was bound to particles, rather than the fluorescent EtBr. (See Figure 3) This specification

enabled the design team to optimize the nanoparticle:RNA ratio.

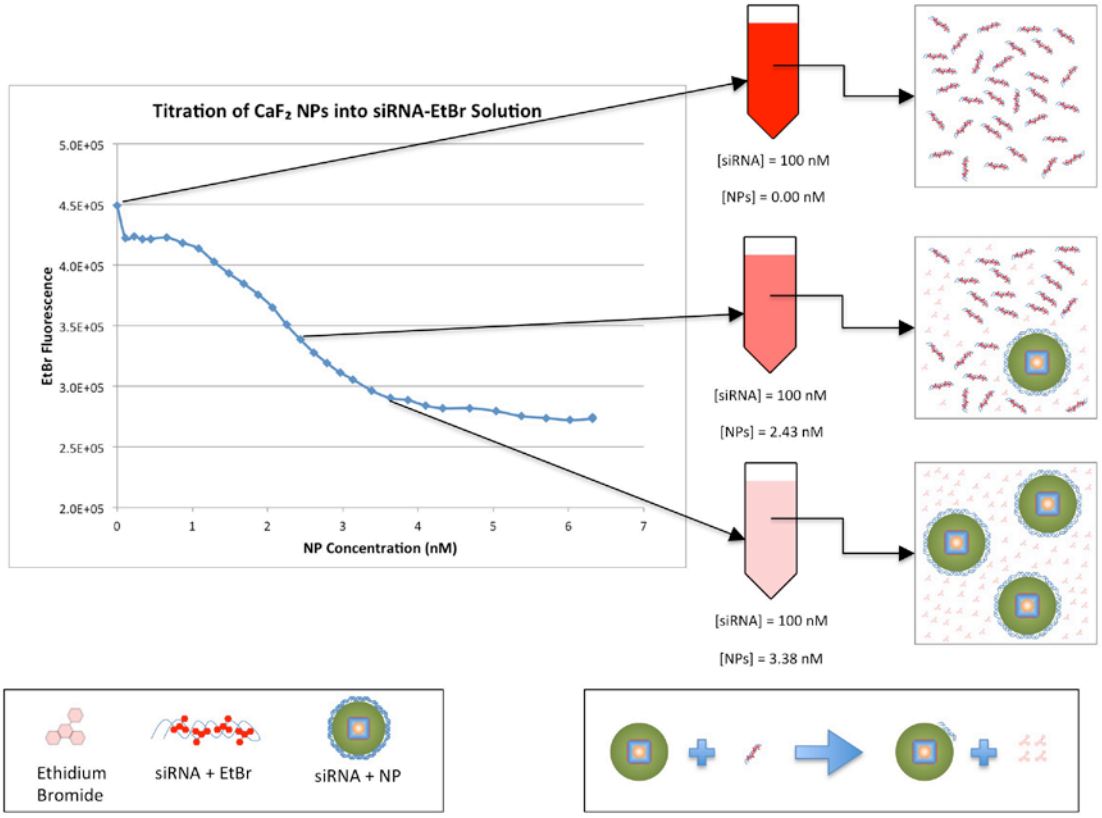

Figure 3: RNA Titration Schematic

Transfection with green fluorescent protein (GFP) plasmid served as a proof-of-concept to test the efficacy of the nucleic acid delivery mechanism and provided a means to directly compare the design to the control, Lipofectamine. In a GFP transfection, plasmid DNA containing the sequence for GFP is taken into the cell. Expression of GFP by the cells produces a measureable fluorescent signal that correlates with transfection, enabling a direct comparison between delivery vectors.

Western blotting, also known as immunoblotting, allows the user to identify and quantify specific proteins in a tissue sample. Samples can be collected following siRNA transfection with experimental and control delivery vectors. After gel electrophoresis and transfer to a nitrocellulose membrane, proteins are identified by interaction with primary and secondary antibodies. The primary antibody binds specifically to the protein of interest. The secondary antibody binds to the primary antibody, which is conjugated with

a reporter, commonly horseradish peroxidase (HRP). When exposed to chemiluminescent agents, the HRP produces a measurable signal. The intensity of the signal can be quantified, and is directly correlated with the quantity of protein. Thus, in the context of gene knockdown, this technique tests both the specificity of the protein and the efficacy of the RNAi mechanism.

The protocols for these tests were developed and finalized through preliminary experiments, and remained consistent throughout the testing of the preliminary, alternative, and final designs. A final comparison and weighing of objectives enabled the design team to select a final design that best meets the objectives, and satisfies all constraints.

Chapter 4: Alternative Designs

Needs Analysis

As discussed in Chapter 2, the only FDA-approved drug regimen for ALS patients is ineffective, justifying the need for a novel therapy. A design that utilizes RNAi to selectively silence mutant SOD1 mRNA will require consideration of several functions. Outlined below, the functions are divided into two categories: primary and secondary. Primary functions are those that fall within the scope of this MQP. Their achievement will be used to measure project success. The secondary functions are those that have potential to be incorporated with the final design, but will not be tested or evaluated in this report.

Primary Functions:

1. Protein silencing

The design must ultimately silence the protein of interest. Research suggests that mutant SOD1 is in part responsible for the motor neuron death associated with ALS. Effectively silencing this protein may provide a therapy to ALS patients.

2. siRNA delivery

To utilize the RNA interference cellular mechanism, the design must deliver siRNA into the cell of interest. Successful delivery is critical to silence the target gene.

3. siRNA protection

Not only must siRNA be delivered, but it must be functional upon entrance into the cell. The design must therefore protect the siRNA from degradation while in the extracellular environment.

Secondary Functions:

1. Deep-tissue imaging

The design should produce a readable signal from within *in vivo* specimens. This feature would allow for particle tracking and confirm that the therapy was delivered to a target location.

2. Cell targeting

The design should be functionalized to target a designated cell type. This would be necessary for *in vivo* applications to deliver the therapy only to cells of interest.

Preliminary and Alternative Designs

Upconverting nanoparticles were identified as the fundamental design platform for their delivery efficacy, imaging potential, and highly tunable surface chemistry. The generic UCNP structure can be divided into three major components; core, shell, and conjugate. The core contains the lanthanide elements responsible for NIR photon upconversion. The shell and conjugate serve to enhance biocompatability and siRNA affinity, respectively.

Variation of the shell and conjugate layers will directly impact the efficacy of the UCNP as a siRNA vector. These components comprise the surface that directly interfaces with the target cells, thus size, shape, charge, and composition are variables to be given consideration. Furthermore, the chemical interaction between shell and conjugate is also of concern; weak bonding can have detrimental effects on cytotoxicity if conjugate polymers dissociate from particle surfaces.

The preliminary nanoparticle incorporates an Yb, Er-doped core. The shell on the particle is a NaYF4 (hexagonal/cubic phase) crystal. Polyethyleneimine (PEI), a branched cationic polymer, was chosen as the conjugate. PEI was electrostatically bound to the particle surface, and is attracted to negatively-charged cell membranes, promoting

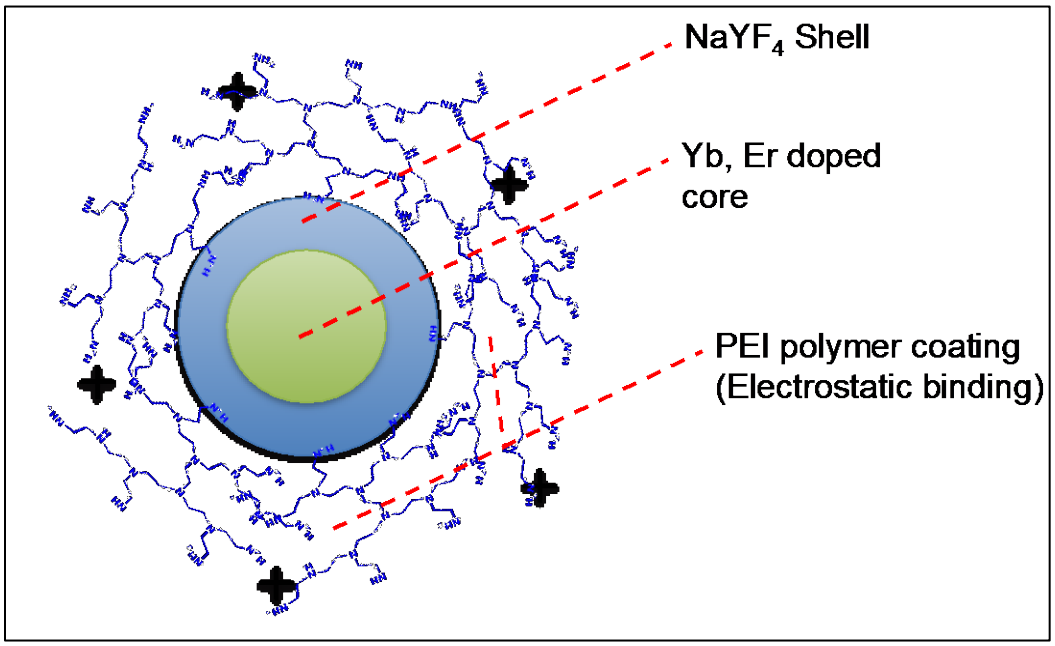

Figure 4: Preliminary UCNP design fabricated by the Han Lab. These particles are $NaYF_4$ core/shell particles with Yb/Er doped cores. The shell is composed of $NaYF_4$. Branched chain PEI was electrostatically bound to the shell as the conjugate to bind siRNA.

endocytosis. Additionally, the cationic property of PEI enables it to bind negatively-charged siRNA, making it an effective (though toxic) transfection agent by itself. Previous experimentation by former rotation students identified the binding ratio as 4 pmol siRNA to 1 µg $NaYF_4$-shell NPs. With DNA plasmid, the mass ratio was optimized at 1 µg to 6 µg $NaYF_4$-shell NPs. See Figure 4 for a schematic of the preliminary UCNP description.

The second alternative design maintained the same core and shell as the preliminary design, with a different conjugate; oleic acid. This conjugate was considered as it has been reported to improve nanoparticle dispersability by increasing the hydrophobicity (Wang, 2003). Dispersability may improve the transfection efficiency, as particle aggregation can limit the efficacy of siRNA

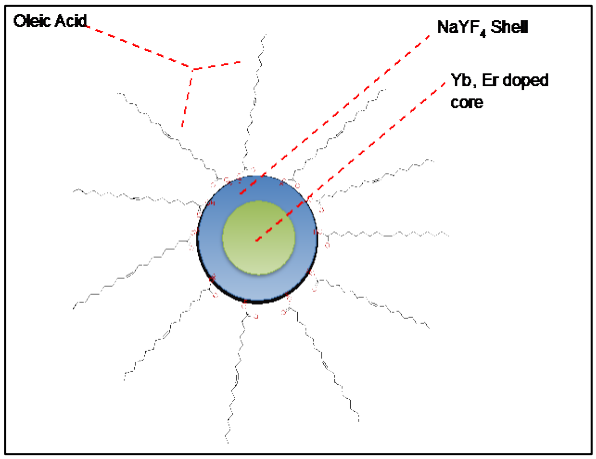

Figure 5: Second UCNP alternative design – Oleic Acid coupled particle

vectors (Alshamsan, 2009). Figure 5 represents a conceptualization of this particle.

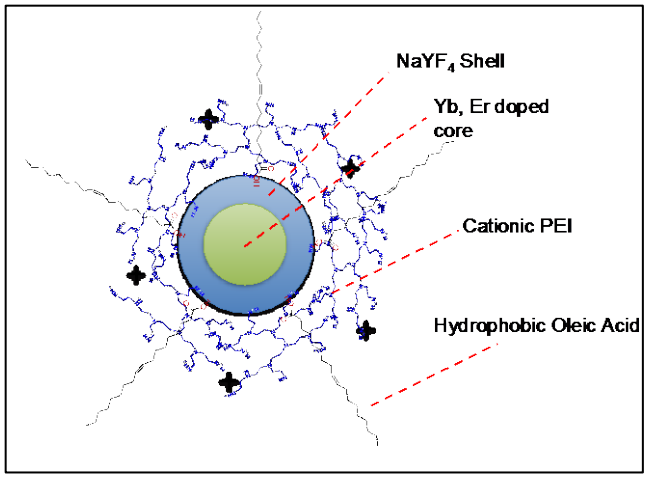

Figure 6: Oleic Acid / PEI coupled UCNP

A third alternative design would combine both PEI and oleic acid onto the same core and shell. The aim of this approach would be to incorporate the desirable properties of PEI and oleic acid; transfection efficacy and dispersability. This would potentially enable the particle to bind with siRNA while minimizing aggregation. A conceptualization of this particle is demonstrated in Figure 6.

A fourth alternative design incorporates a new shell around the same lanthanide doped core; CaF_2. The surface chemistry associated with this shell provides one critical difference from the $NaYF_4$-shell; it can bond with PEI polymers covalently rather than electrostatically. This alternative may enable the use of PEI for its suitable transfection properties, while improving the biocompatibility of the UCNP. Figure 7 represents this particle.

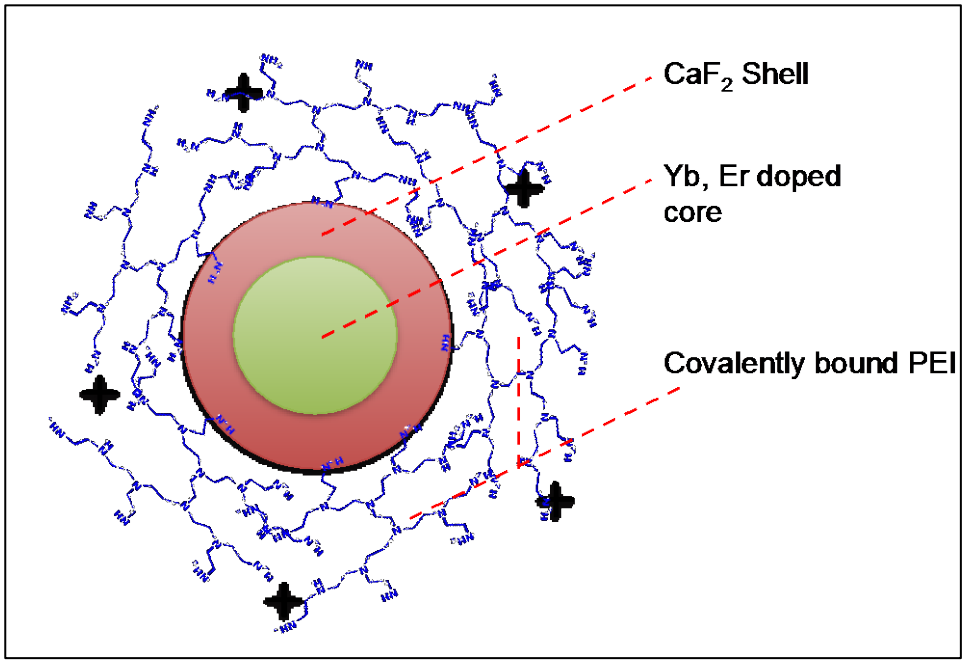

Figure 7: Calcium fluoride shell UCNP with PEI

Preliminary Data

Several experiments were conducted to ensure the feasibility of the proposed design. These preliminary studies also served as a learning platform for the design team, and an opportunity to develop and customize all laboratory protocols. All *in vitro* experiments were performed using the HeLa cervical cancer cell line. Cells were cultured using Dulbecco's Modified Eagle Medium (DMEM) at 5% CO_2 and 37°C incubation. All nanoparticle stocks were synthesized and purified by Han Lab. For details on the synthesis, see Manufacturability of UCNPs in Chapter 6: Discussion.

The following tests (GFP-Plasmid Transfection, MTT cytotoxicity, and Western Blot) each provide quantitative measurements of how well the design meets the objectives. Preceding each figure, a brief discussion will outline the experimental method and interpretation of the data.

Preliminary MTT Cytotoxicity Assay

To assess nanoparticle cytotoxicity, an MTT assay was performed using Promega's CellTiter® 96 Non-Radioactive Cell Proliferation Assay according to the manufacturer's instructions. Plated cultures were prepared on standard tissue culture polystyrene 96-well plates. Cells were seeded at a density of 7,500 cells/well in DMEM + 10% FBS, and incubated 24 hours before sample exposure. During sample loading, growth medium was aspirated and replaced with Gibco's low serum Opti-MEM. $NaYF_4$-shell nanoparticles were loaded into wells at increasing concentrations and incubated for 4 hours. As a comparison, $NaYF_4$-shell particles were also mixed with plasmid and given 5 minutes to complex prior to loading. Medium was then aspirated and replaced with DMEM + 10% FBS and cells were incubated for 24 hours. MTT dye (15 µL) was added to each sample well. After 4 hours, 100 µL of solubilization solution was added to each sample well. As instructed in the protocol, the plate was sealed with parafilm and left for 24 hours at RT before measuring absorbance to allow the MTT salt to convert to its formazan product. Absorbance was read at 570 nm. For each concentration tested, n = 8.

Figure 8 displays the results of two separate MTT assays. The toxicity of the preliminary $NaYF_4$-shell nanoparticle correlates with cell viability and is measured

against particle concentration. On the x-axis, particles are measured in micrograms per square centimeter of the tissue culture surface. Relative percent viability is a measure of cell viability compared to a control group (unexposed to nanoparticles). The data shown in red represents plasmid-coupled nanoparticles. The nanoparticles and plasmid form complexes through electrostatic stacking interactions. The plasmid-nanoparticle complexes were formed using the GFP Transfection protocol. The data in green represents unbound particles.

The data suggests that UCNP-plasmid interaction decreases nanoparticle cytotoxicity, in which is suggested by the plateau-like trend in the data. The data represented by the green line indicates that toxicity directly increases with particle concentration, as evidenced by the constant, negative slope that approaches <20% initial cell viability at concentrations greater than 26.67 micrograms of nanoparticles per square centimeter. The data represented by the red line indicates that the binding of DNA plasmid decreases the toxic effect of the nanoparticles. (Note: these two experiments were done on different plates but at the same time and under the same conditions)

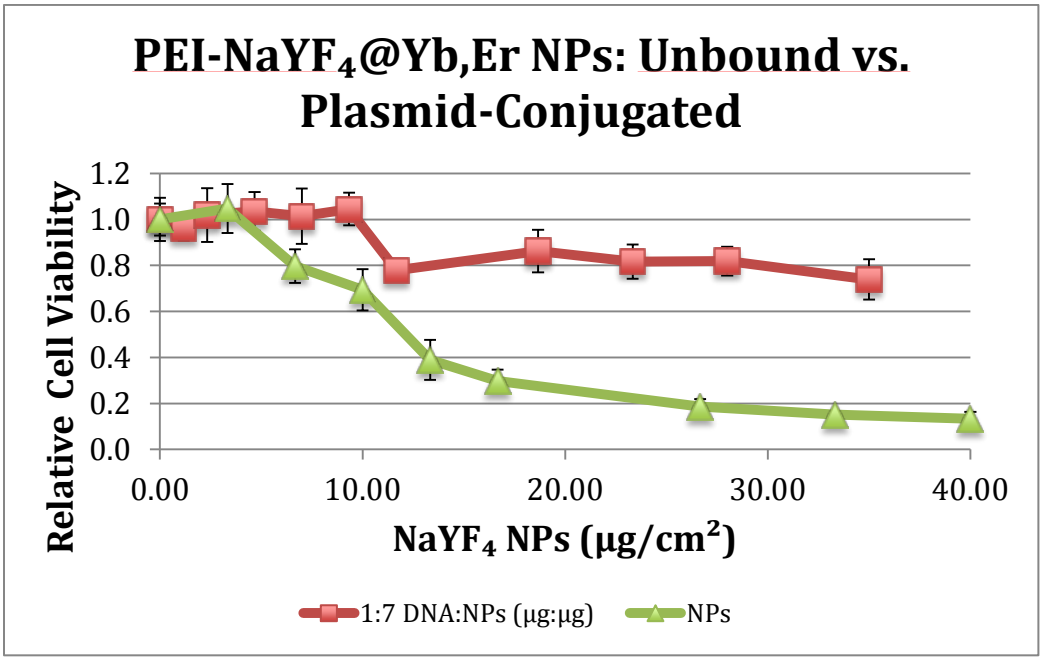

Figure 8: Preliminary MTT cytotoxicity

GFP Plasmid Transfection

To quantify the efficiency of the preliminary $NaYF_4$-shell nanoparticle, GFP plasmid transfection experiments were conducted in 96-well plates. The intensity of GFP fluorescent signal should correlate directly with transfection efficiency. Cells were seeded at densities of 7,500 cells/well in DMEM + 10% FBS, and incubated 24 hours prior to sample loading. During transfection, medium was aspirated and replaced with Gibco's low serum Opti-MEM. Exposure time was 4 hours incubation, at which point medium was aspirated and replaced with DMEM + 10% FBS. Cells were incubated with plasmid for 48 hours. Before loading, plasmid was mixed with nanoparticle solution and allowed 20 minutes to form complexes. For Lipofectamine, 20 minutes was also allowed. GFP fluorescence was read at 24- and 48-hour time points. Figure 9 shows data from the 48-hour reading. Each group was performed in octet for and n of 8.

Transfection with GFP plasmid serves as an evaluation of transfection efficiency. In this experiment, GFP plasmid concentration was fixed at 12 μg/mL and transfection was performed with the $NaYF_4$-shell nanoparticles (84 μg/mL) and the control agent, Lipofectamine. The fluorescence intensity directly correlates with transfection efficiency.

In Figure 9, the y-axis represents the fluorescence for the samples, which is relative to the PBS control. This serves as an indication that the preliminary design achieves transfection efficiency at a level that is approximately 45% of that achieved using a liposomal delivery method.

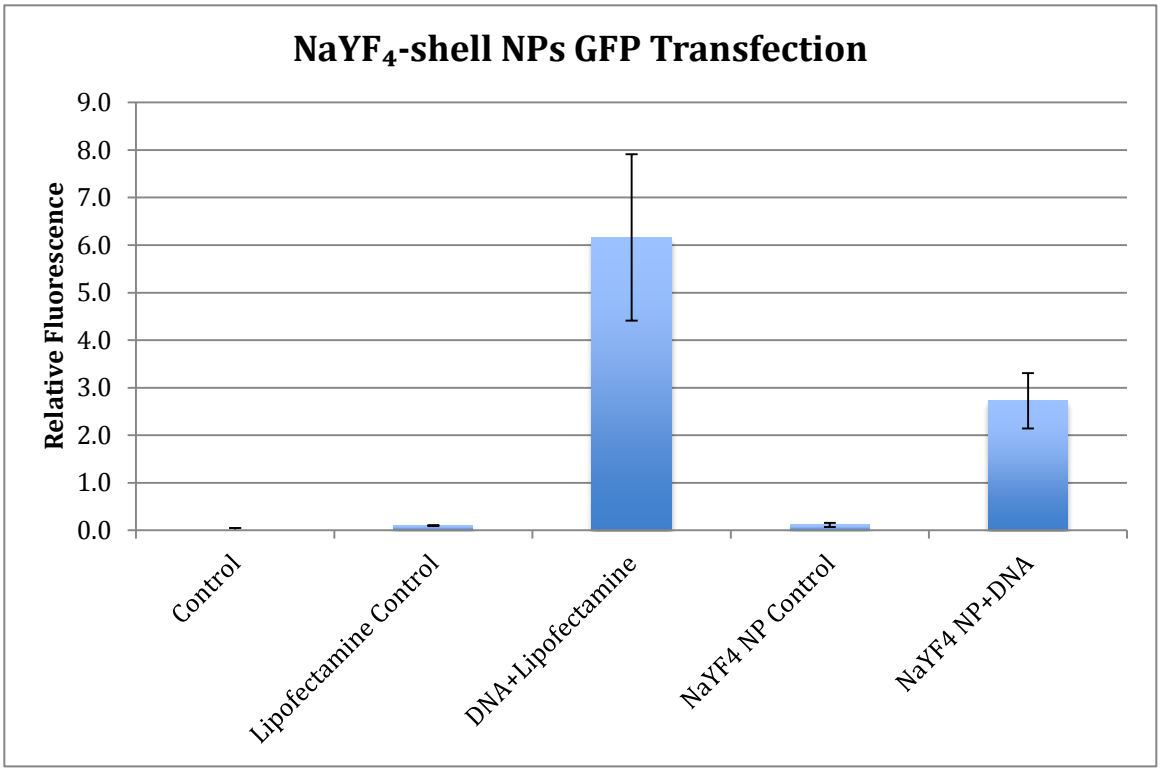

Figure 9: Quantification of preliminary GFP plasmid transfection

Western Blot Analysis

For Western blotting, samples were prepared from transfected cell populations cultured in 12-well plates. Cells were seeded at 90,000 cells/well in DMEM + 10% FBS and incubated 24 hours prior to transfection. Upon loading, media was aspirated and replaced with Gibco's low serum Opti-MEM. Samples were prepared for PBS controls (100 µL), NP controls (7.5 µg), and a fixed NP-siRNA experimental treatment (7.5 µg to 30 pmol). The samples were exposed to cells for 4 hours incubation, and then aspirated. Cells were left to incubate 72 hours before lysis and protein harvest. Lysis was performed using 200 µL Promega M-PER lysis buffer per well. The lysis buffer was supplemented with Thermo Scientific's Halt Protease Inhibitor Cocktail. Samples were purified by micro centrifugation and stored at -20° C. Sample concentration was determined via Pierce BCA Assay and normalized during gel loading.

A sample volume of 24 µL was added to 6 µL Lammeli loading buffer, for a total gel loading volume of 30 µL. Gel (10% SDS-PAGE) electrophoresis was run at 70V for

130 minutes. Nitrocellulose was used for the transfer membrane, and transfer was conducted at 100V for 1 hour. Membranes were washed 3 times with PBS-Tween (PBST), and blocked in 5% milk-PBST for 1 hour prior to primary antibody incubation.

Primary antibodies were added at 1:5000 and 1:500 dilutions for α-Tubulin (Sigma Aldrich, 010M4813) and SOD1 (Meridian, K90077C), respectively. Incubation occurred at 4^{O} C for 24 hours. Blots were then washed in PBST, and incubated 1 hour in 5% milk-PBST at room temperature. Dilutions for secondary antibodies were 1:10,000 for both proteins. Following secondary incubation, blots were washed in PBST a final time, and exposed with SuperSignal® West Pico Chemiluminescent substrate (Thermo Scientific, #34080). Imaging was completed with an ImageQuant LAS 4000 system. To analyze protein knock down, a ratio is calculated between the protein of interest (SOD1) and the control protein (α-tubulin). This accounts for the natural variation of protein concentration between samples, and enables calculation of a normalized, quantitative value for knockdown.

Figure 10 is one example (of 5 trials) of a Western blot membrane after chemiluminescent imaging. For each sample (three for each parameter) the top band represents α-tubulin, while the lower set of bands represent SOD1. One can see qualitatively that the bands in the experimental UCNP-siRNA lanes are less intense than those of the control samples. This serves as an indication that knockdown was achieved.

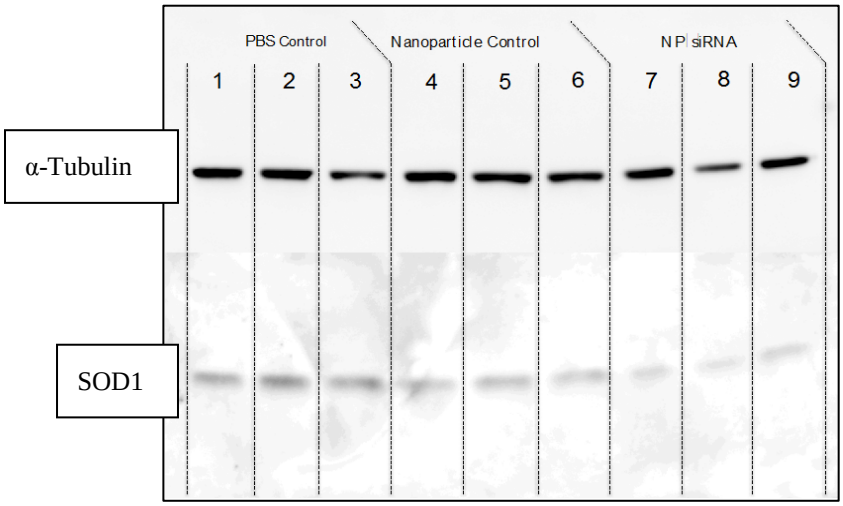

Figure 10: Western blot from transfection with 7.5 µg $NaYF_4$ -shell particle

Further analysis using ImageJ software was used to quantify band intensities. Each lane can be the measured independently for the intensity of the signal, which appears as a peak (black) in a background baseline signal (white). The area of the peak correlates directly with band intensity, enabling quantification of band intensity. Figure 11 displays the relative, average intensities for each sample set, and confirms the indication that SOD1 knockdown was achieved; approximately 55% less than a PBS control. This is not only a measure of design efficacy, but also its specificity; as SOD1 target protein expression appears to be inhibited.

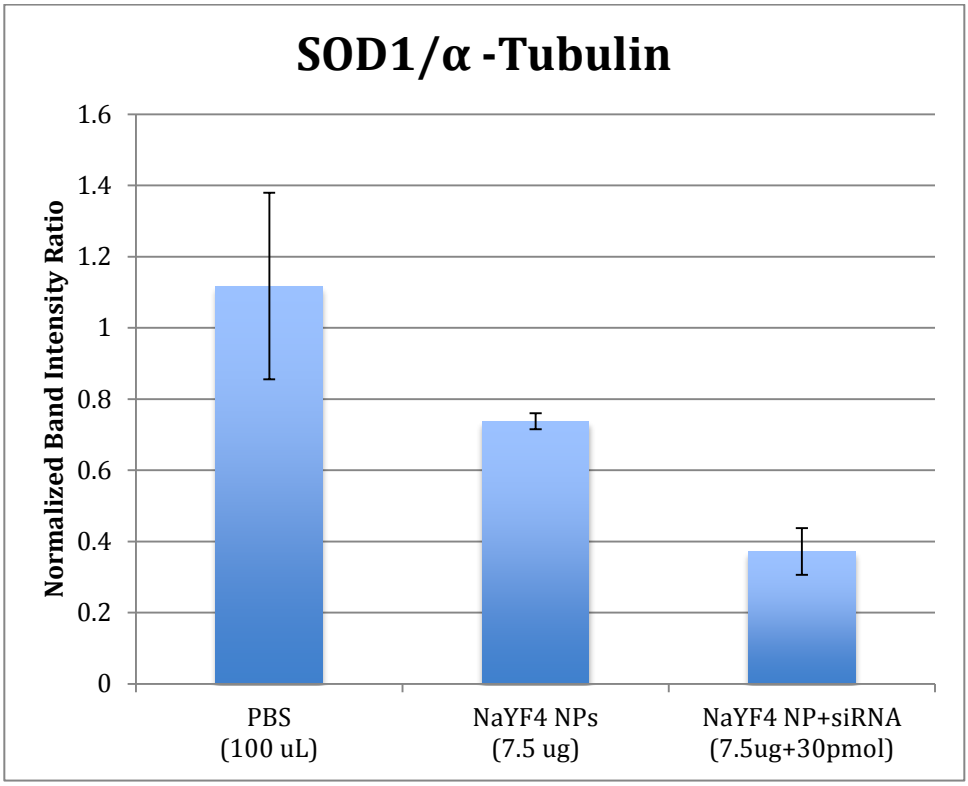

Figure 11: Quantification of SOD1 protein bands from Western blot shown in Figure 10. Each bar represents the average of 3 samples. Error bars represent 1 standard deviation from the average.

Chapter 5: Design Verification

Included in this chapter are the results of the experiments performed using the final nanoparticle design, the CaF_2-shell nanoparticles. The CaF_2 shell was hypothesized to offer increased biocompatibility, while still serving as an effective transfection agent. In the chronological order they were performed, the results include cytotoxicity data, plasmid binding ratio optimization, siRNA binding ratio optimization, GFP plasmid transfection, and SOD1 siRNA transfection with Western blotting. Following each data figure, key quantitative features will be highlighted.

The order in which these experiments were conducted was intentional. Cytotoxicity provided grounds for identifying the acceptable dose of CaF_2-shell UCNPs to be used in transfection experiments. Binding ratio optimization was conducted prior to transfections to optimize the efficiency and delivery of the system. Having identified the acceptable toxic range and optimal particle conjugation, transfections could be performed with nanoparticle and siRNA doses which best met the design objectives of safety and efficiency. The objectives of efficacy and specificity were then evaluated with the GFP and siRNA transfection assays, respectively.

Cytotoxicity

CaF_2-shell NPs were added in concentrations of 10, 20, 30, 50, 100, 150, 200, 500, and 1000 ug/mL to obtain data on a logarithmic scale. Cell viability was measured relative to a

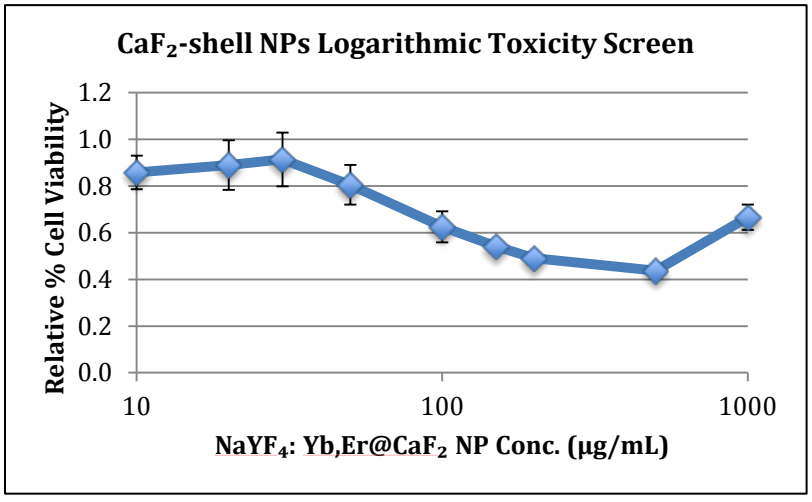

Figure 12: Final MTT cytotoxicity

control that received only PBS in lieu of NPs during loading. This data is shown in Figure 12.

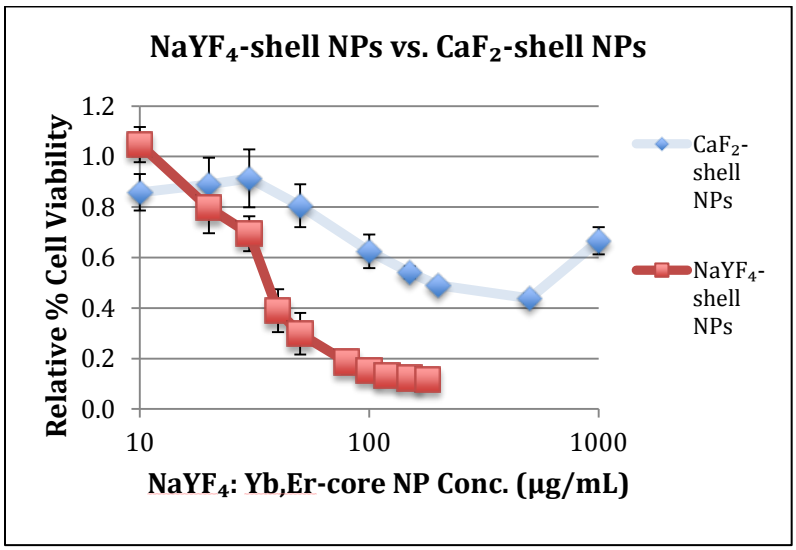

Figure 13: Comparison - final and preliminary toxicity

In Figure 13 the data from CaF_2-shell NP cytotoxicity experiments is compared with previous data from $NaYF_4$-shell NP data from Figure 8 (note: experiments were performed independently). The data demonstrates that $NaYF_4$-shell NP resulted in a more rapid decrease in cell viability as a function of nanoparticle concentration. For example, at a concentration of 30 µg/mL, cell viability with the $NaYF_4$-shell particle measured 69%. At this same concentration with the CaF_2-shell particle, the viability measured 91%.

Binding Ratio Optimization - DNA

Optimization of the Plasmid-NP binding ratio was determined via agarose gel electrophoresis. A 3% agarose gel was prepared in Tris-Acetic acid EDTA (TAE) with 1 µL EtBr stock solution (10g/L). Two microliters of 6X Lammelli loading buffer was added to each sample. Samples were prepared in which mass:mass ratios between CaF_2-shell UCNPs and plasmid DNA increased. The ratios (DNA:NP) evaluated were: 1:10, 1:20, 1:30, 1:40, 1:50, 1:60, 1:70, 1:80, and 1:90. A plasmid DNA only (no NP) control was loaded in lane 1. For each sample, 20 µL was loaded into each lane. Two µL EtBr stock solution was added to the TAE running buffer, and the gel was run at 70V for 45 minutes. Fluorescent imaging was conducted

with an ImageQuant LAS 4000 system. The image can be seen in Figure 14. Results were prepared using ImageJ and Microsoft Excel®.

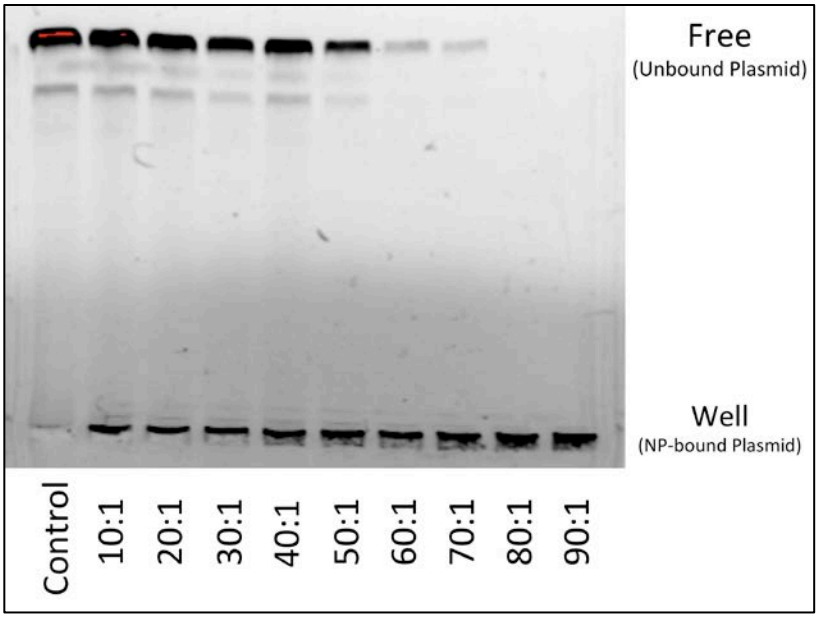

Figure 14: Mass binding ratio of DNA plasmid to CaF2-shell NPs

At the top of each lane, free (unbound) DNA appears as a visible band. When UCNPs bind DNA plasmid, the complex is too large to travel through the agarose gel, and remains in the well; the bands at the bottom of the gel. As the ratio approaches optimal binding saturation, DNA band intensity decreases as the quantity of free DNA decreases. As a result optimal binding occurs near the lane in which the free DNA signal is no longer detectable – which appears to occur at the 1:80 ratio. Figure 15 demonstrates an ImageJ quantification of the band intensity for free DNA.

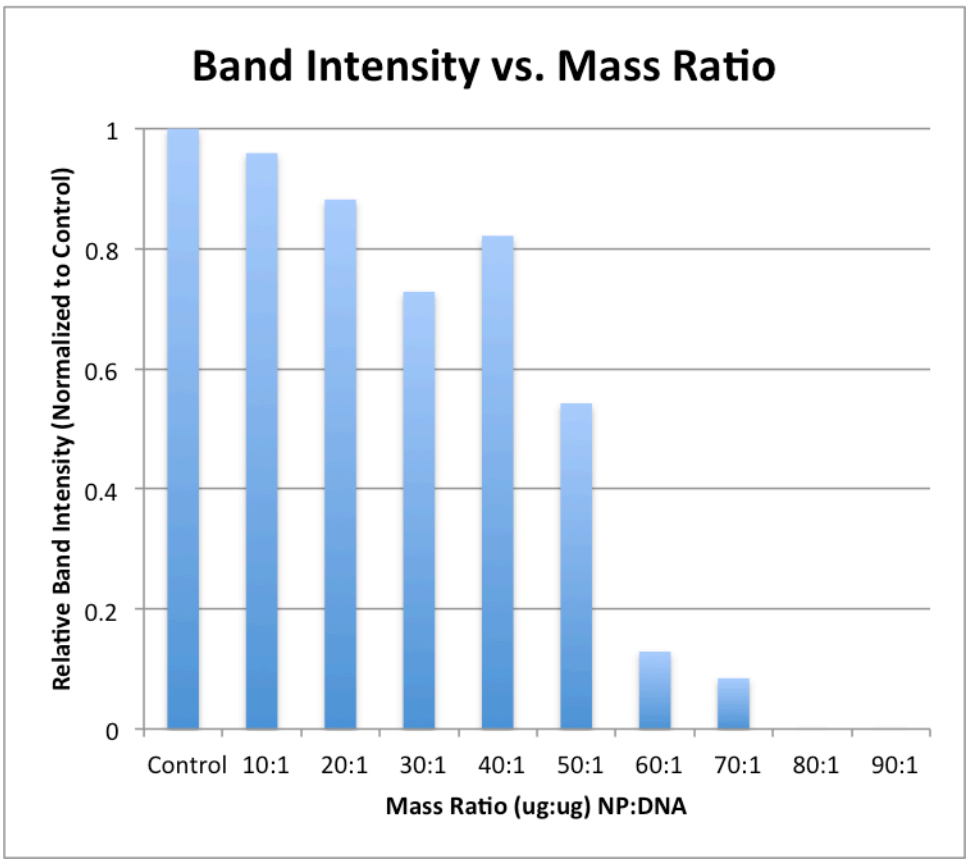

Figure 15: Quantification of NP-Plasmid agarose gel

Binding Ratio Optimization - siRNA

Optimization of the NP-siRNA binding ratio was determined via NP titration into an Ethidum Bromide – siRNA solution. Ethidium bromide (2 µL of [1 mM] solution) was complexed with siRNA (10 uL of [20 uM] solution) in 1.998 mL PBS in a standard cuvette. A stock solution was prepared of equal EtBr and siRNA concentrations, and 2 µL UCNPs (0.1g/L). Titration was performed by adding stock solution to the cuvette in 10 µL increments (larger increments could be used in the plateau regions of the plot) until sample fluorescence reached a minimum. Fluorescence was measured using a FluoroLog™ spectrofluorometer, at an excitation wavelength of 545 nm. Emission was recorded at 590nm. Titration was discontinued after fluorescence reached a steady minimum and results were prepared using Microsoft Excel®.

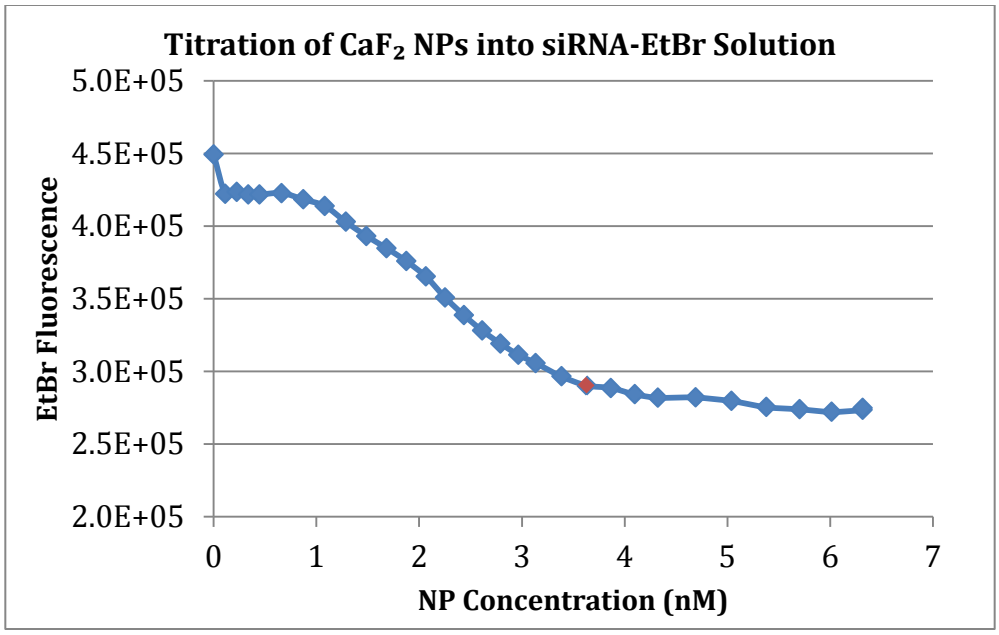

Figure 16: NP titration in siRNA-EtBr solution

As shown in Figure 16, at 3.6 nM (marked in red) the plateau phase of minimum fluorescence is reached. This minimum indicates that a maximum quantity of EtBr has been released and thus inactivated. Because the EtBr is released as siRNA binds to particles, this represents the point at which the optimal siRNA- CaF_2-shell UCNP ratio is reached.

Plasmid transfection

GFP plasmid transfection was performed using CaF_2-shell UCNPs in varying ratios between 1:60 and 1:70 µg DNA : µg CaF_2-shell UCNPs. Negative controls were prepared with PBS, CaF_2-shell UCNPs only, DNA only, and Lipofectamine™ only. The positive control was prepared with Lipofectamine™ and DNA. The most notable result was that the NP transfection groups showed no fluorescence beyond that of the NP control, as seen in Figure 17.

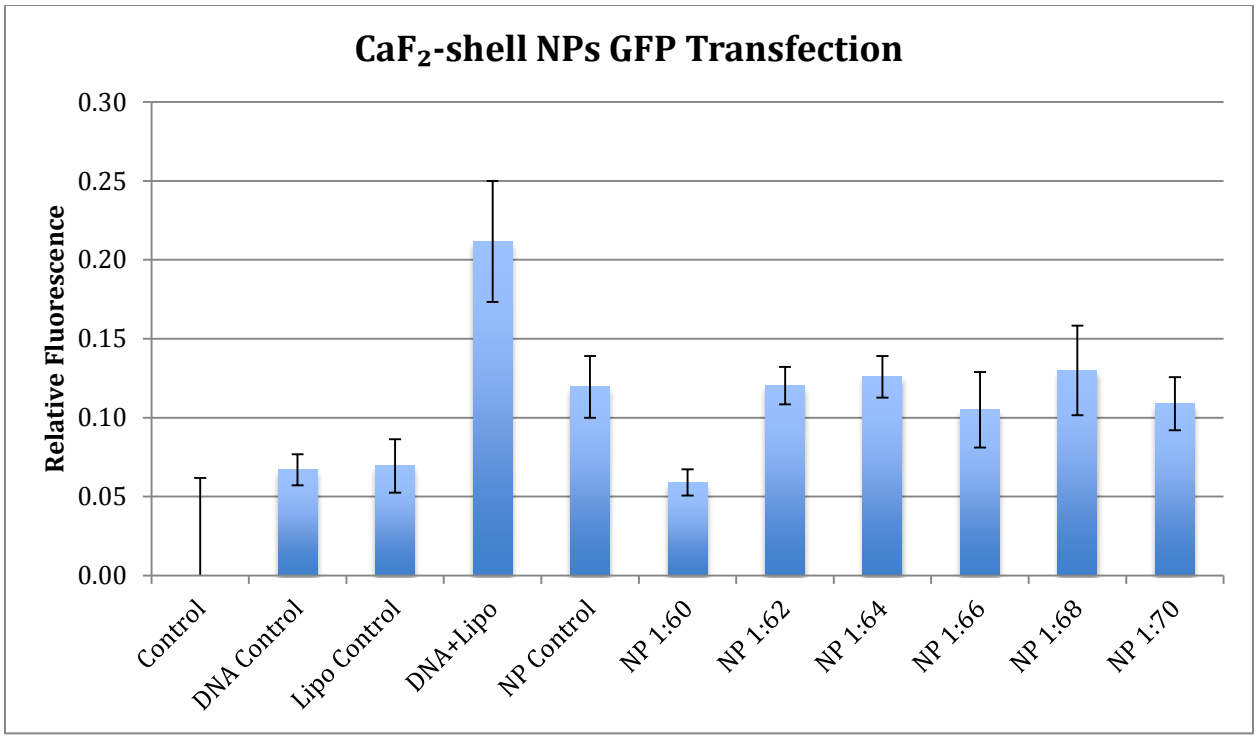

Figure 17: Quantification of final GFP plasmid transfection

siRNA Transfection, Western Blot

Transfection was performed under the same conditions as the preliminary trial in Chapter 4 (Figure 11). The cells were incubated with the transfecting agents for 4 hours, and were allowed 72 hours incubation before sample harvest for Western blotting. In addition to the negative and positive controls, NPs were tested with a fixed RNA quantity of 30 pmols. The ratio was identified from the binding ratio optimization experiment where the optimal molar ratio 1NP : 30 siRNA was derived. For comparison, two other ratios were employed; ½ and 1½ times the optimal NP quantity. For each ratio or control, an n = 2 samples was used. Sample concentrations were confirmed via BCA assay and 13.3 ug per sample was loaded into the gel (30 uL loading volume).

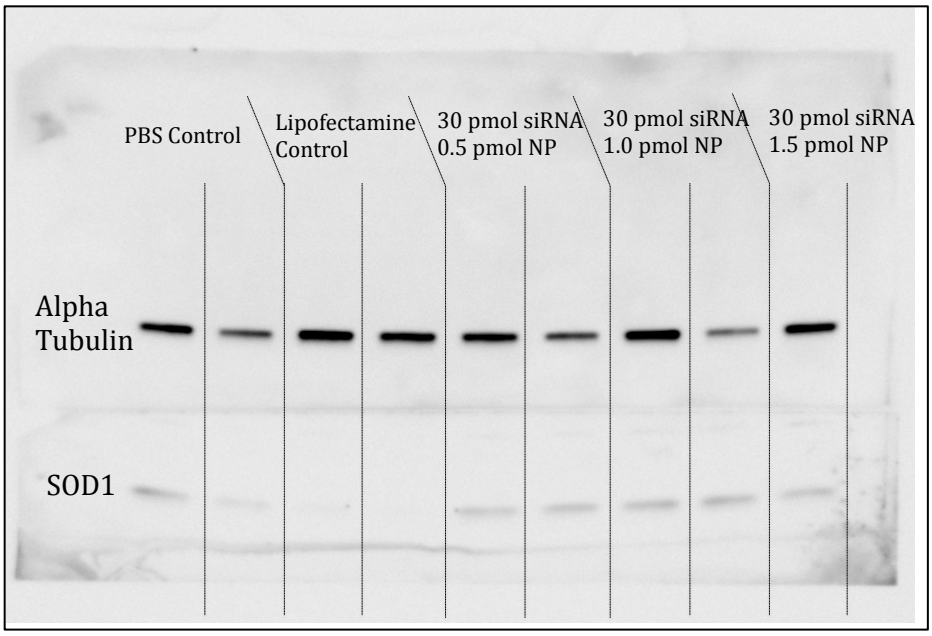

Figure 18: Western blot with final design

Qualitatively in Figure 18, a visible decrease in band intensity for the positive control lanes transfected with Lipofectamine™ occurred, although knockdown did not appear to be achieved with the nanoparticle transfection. Band intensity was quantified using ImageJ software, and knockdown evaluated as the ratio of SOD1 per the control, alpha-tubulin.

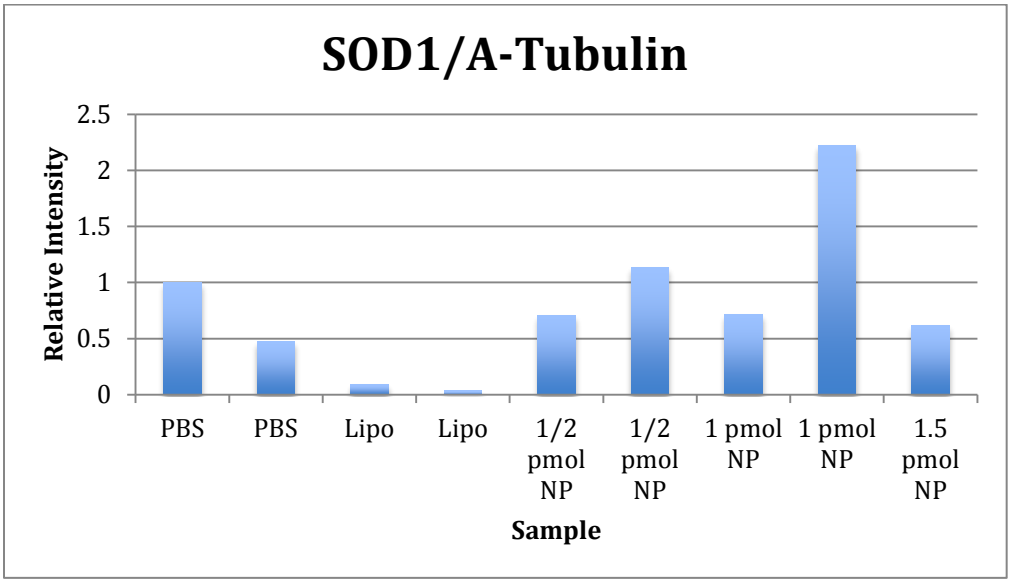

Figure 19: Quantification of final western blot

As shown in Figure 19, quantification suggested that SOD1 knockdown was not achieved with the CaF_2-shell nanoparticles at any of the tested ratios. Follow up testing was conducted in an effort to obtain stronger chemiluminescent signaling, and reduce background noise. A new protocol was used to obtain samples of higher protein concentration, and a 15% polyacrylamide gel was utilized to allow better separation of the SOD1 protein.

Samples were prepared in 6-well culture plates, lysed using 400 µL Laemmli's reducing buffer (2X), and were scraped off the plate using a spatula. Before gel loading, samples were ultra-sonicated. An adeno-associated virus carrying SOD1 gene was incorporated as a negative control in addition to the standard PBS control. The incubation period was reduced to 24 hours (instead of 72) due to time constraints. All other preparations were kept constant.

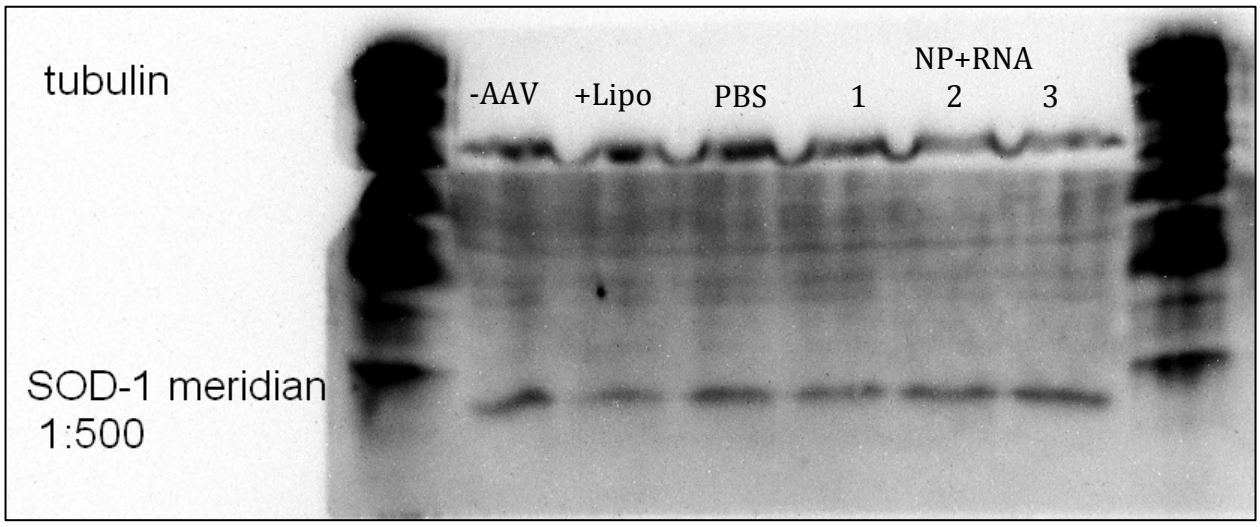

Figure 20: Western blot with modified protocol

Figure 20 represents the blot prepared with the modified method. Band intensity for SOD1 was improved, although the background signal was relatively high. In addition the tubulin control bands were not clear because they remained in the stacking section of the gel. Most importantly, the SOD1 bands do not appear to exhibit any knockdown; similar to the result in Figure 18.

Chapter 6: Discussion

In order to assess the characteristics of the different UCNP designs in terms of the objectives, each UCNP design was placed through a number of different experiments as detailed in the previous chapter. Each of these experiments is paired with a different objective. By bringing together the data from the different experiments, it is possible to evaluate the viability and effectiveness of the UCNP design as a transfection agent. In the following sections, UCNPs are discussed as a possible ALS treatment in terms of their economic, environmental, social and even political impact; safety, ethics, and sustainability; and manufacturability.

Viability as Transfection Agent

Both UCNP designs were tested for toxicity using the MTT as an indicator of live cells. The more cells alive 20 hours after a 4-hour incubation, the less toxic the effect. The range of toxicity was then compared to the dosages needed for transfection to determine whether the UCNP is a viable option in terms of safety, defined as 90% viability of the cells or greater.

During the preliminary testing, $NaYF_4$:Yb,Er@$NaYF_4$ core/shell nanoparticles ($NaYF_4$-shell NPs) with a PEI coating were used for transfection. Cell viability of these particles showed a sharp drop-off beyond a concentration of 10 μg/mL, as shown in Figure 8. At concentrations of 20 μg/mL or more, only 80% of the cells were still metabolically active within 20 hours of exposure to the $NaYF_4$-shell NPs. Given the high concentrations typically needed for DNA transfection, this data seems to rule out these preliminary particles as a viable DNA transfecting agent. However, siRNA does not require such high doses, which allows for $NaYF_4$-shell NPs to be assessed as a siRNA delivery system.

The binding ratio for $NaYF_4$-shell NPs with DNA plasmid was experimentally determined as 7:1 by mass to achieve effective transfection of DNA plasmid. The concentration of DNA plasmid used during transfection in a 96-well plate is 5 μg/mL. In order to transfect that concentration of DNA plasmid, 70 μg/mL of $NaYF_4$-shell NPs was used. The cell viability at this high concentration for $NaYF_4$-shell NPs alone is less than 20%. However, complexing of the particles to DNA seemed to have a protective effect. As seen in Figure 8, cell viability seems to plateau around 80% for $NaYF_4$-shell NPs complexed to DNA plasmid at concentrations ranging

from 35 to 105 μg/mL. This accounts for the positive transfection results seen in Figure 9. GFP expression was observed using $NaYF_4$-shell NPs for transfection at DNA concentrations ranging from 5 to 25 μg/mL.

The binding ratio for $NaYF_4$-shell NPs with siRNA was experimentally determined to be 1:4 μg NPs to pmol siRNA to achieve effective knockdown. The concentration of siRNA used during transfection in a 12-well plate was 15 nM. In order to transfect that concentration of siRNA, 3.75 μg/mL of $NaYF_4$-shell NPs needed to be used. The cell viability at this low concentration is well over 90% for $NaYF_4$-shell NPs alone, therefore cell viability when using $NaYF_4$-shell NPs for siRNA transfection should be above the acceptable threshold of 90%.

During the verification process for the final design, $NaYF_4$:Yb,Er@CaF_2 core/shell nanoparticles (CaF_2-shell NPs) conjugated to a citric acid-PEI coating were used for transfection. Cell viability for these particles showed a less dramatic drop-off beyond a concentration of 80 μg/mL than $NaYF_4$-shell NPs as shown in Figures 12 and 13. At concentrations lower than 80 μg/mL, the cell viability for CaF_2-shell NPs seems to stabilize around 80%. Cell viabilities of less than 20% were not observed until the concentration exceeded 150 μg/mL. This reduced toxicity at high concentrations enables a greater range of dosages for CaF_2-shell NPs for both DNA and siRNA transfection.

The binding ratio for CaF_2-shell NPs with DNA plasmid was experimentally determined as 80:1 μg NPs to μg DNA for maximal binding. Typically, the most effective ratio for transfection is somewhere beyond this point. As mentioned above, the concentration of DNA plasmid used during transfection in a 96-well plate is 5 μg/mL. In order to transfect that concentration of DNA plasmid, at least 350 μg/mL of CaF_2-shell NPs would need to be used. The cell viability at this high concentration for CaF_2-shell NPs alone is less than 20%. It is possible that the complexed DNA plasmid would have a similar protective effect for the cells as seen with the $NaYF_4$-shell particles. Prior to determining the binding ratio of DNA plasmid to CaF_2-shell NPs, a preliminary MTT assay was run using the binding ratio of the $NaYF_4$-shell particles, 1:7. The data is shown in Figure 8. A similar protective effect was seen at CaF_2-shell NP concentration ranging from 5 to 100 μg/mL. However, since the binding ratio used during transfection may be much higher, it cannot be definitively stated that this would be the case.

The binding ratio for CaF_2-shell NPs with siRNA was experimentally determined to be at a 1:30 molar ratio for maximal binding. The average concentration of siRNA used during transfection in a 12-well plate is 15 nM. In order to transfect that concentration of siRNA, a CaF_2-shell NPs concentration of at least 0.5 nM would need to be used, which is equivalent to 22 μg/mL. The cell viability at this low concentration is around 89% for CaF_2-shell NPs alone, therefore cell viability when using CaF_2-shell NPs for siRNA transfection is close to the acceptable threshold of 90%.

When comparing the two particles, the CaF_2-shell NPs are less toxic at a higher concentration but have a greater toxicity overall in that cell viabilities never exceed 90% whereas $NaYF_4$-shell NPs have high toxicities at lower concentration but do have a small window where cell viability is greater than 90%. The complicating factor becomes the protective effect of the NP-nucleotide complex. If this protective effect is seen in both particles types and extends to both types of nucleic acid, then both the initial and final particle designs could be viable as transfection agents based on their toxicities. More testing is needed to demonstrate this experimentally. From here, it is necessary to compare the particles based on other objectives, namely specificity, scalability, and efficacy.

Effectiveness as Transfecting Agent

After determining the working range of each particle design, it was necessary to evaluate the effectiveness of each particle by performing transfections using both DNA plasmid and siRNA. Once maximal binding ratios were established, transfections were performed using those ratios of nucleic acid to nanoparticles and higher ratios in order to find the ratio with maximal transfection efficiency. If this was found, further transfections were performed to find the optimal DNA concentration for transfection. This was then compared with a commonly used transfection agent, Lipofectamine™2000.

For $NaYF_4$-shell NPs, the binding ratio with DNA plasmid was experimentally determined as 7:1 μg of NPs to μg of DNA. This was determined prior to the design team taking on the project. As seen in Figure 8, measurable expression of GFP was observed with this ratio. GFP expression was used to indicate that the nucleic acid in complex with the particle is being transfected into the cell, is being released, and is still functional. Since there is a significant

amount of fluorescence beyond the background of particles alone, it can be inferred that the $NaYF_4$-shell NPs effectively deliver nucleic acid into the cell and may protect it from degradation. Once inside the cell, the particles are also releasing the DNA plasmid since it cannot be transcribed unless it is free.

With the CaF_2-shell NPs, a binding ratio of 80:1 μg NPs to μg DNA was determined via agarose gel (Figures 14 and 15). As seen in Figure 17, there was no measurable expression of GFP since the relative fluorescence is of the same magnitude as the NP control. This suggests that CaF_2-shell NPs are getting into the cell since the background fluorescence of the particle is seen in both the NP control and the NP+DNA group. However, since GFP fluorescence was not observed beyond the fluorescence of the particle, GFP does not appear to be expressed - either because the DNA plasmid is not being released from the particle, or because it is being degraded before it can be expressed.

A similar situation is seen for siRNA transfection measured as SOD1 knockdown (Figures 10, 11, 18, 19, and 20). The $NaYF_4$-shell NPs show effective transfection with a 45% knockdown of SOD1 ($p<0.01$) compared to the control. This shows effective delivery and protection of the siRNA. In contrast, the CaF_2-shell NPs show no significant difference between the control group and the NP+siRNA group. This suggests that either the siRNA is not being released or is being degraded. It seems more likely that the CaF_2-shell NPs are simply not releasing the nucleic acid because the binding ratios are so much higher. This shows a much greater affinity of nucleic acid for particle. However, further testing would need to be done to test this hypothesis.

A proposed mechanism of release that would explain this situation is electrostatic stacking interactions that are strong enough to overcome the pH changes within the cell. Nucleic acid is complexed to the particles through electrostatic stacking interactions. The negatively-charged nucleic acids are attracted to the positively-charged particle surface. The particles then shield the negatively-charged nucleic acids from the negative surface of the cell, which allows the particle-nucleic acid complex to enter into the cell via endocytosis. Once inside the cell, the particle-nucleic acid complex would be exposed to lysosomes, which alter the pH within the endosome. With the $NaYF_4$-shell particles, this pH change may have been enough to liberate the nucleic

acid. However, with the CaF_2-shell particles, this pH change does not seem to overcome the stacking interactions.

UCNPs as an ALS Treatment: A larger perspective

Economics

As presented earlier, the only drug currently approved for treatment of ALS is Riluzole. Even with questions concerning its efficacy, the cost is unfavorable at roughly $17 per 50 mg pill, prior to insurance coverage. (Epocrates, 2012) If siRNA can be effectively delivered into motor neurons using UCNPs, the market value of this treatment is potentially beyond that of Riluzole. It is impossible to estimate exact figures for such a treatment.

Environmental Impact

With any new therapy, it is important to understand downstream effects of the disposal not only of the therapy itself but also of the materials associated with its manufacturing. The production of UCNPs requires the use of lanthanide salts. Ytterbium, erbium, and thulium, the current compounds used for doping, pose no environmental threat to plants or animals. They are considered biologically inert. Water-soluble compounds of yttrium are considered mildly toxic, mostly affecting aquatic animals. Therefore waste disposal in the manufacturing process would need to be monitored but no special licensing or permits need to be acquired. (Ytterbium Oxide, 2010) (Erbium Oxide, 2008)

Societal Influence

ALS is a devastating disease that affects approximately 6,000 people in the U.S. annually. The development of a treatment for ALS would not only save the lives of these people but also reshape the lives of their families and friends. A siRNA delivery system could provide hope to thousands of people who are currently listed as terminal.

Political Ramification

Until recently, ALS was rarely given much attention by the public. The most common association is with Major League Baseball Hall of Famer Lou Gehrig, who retired from the game at the age of 36 because of the disease. However, in early 2011, former Massachusetts Governor Paul Cellucci was diagnosed with a slow progressing form of the disease bringing ALS to the forefront of the public attention. Governor Cellucci has put forward the goal of raising $10 million for ALS research at UMass Medical School in Worcester. (Phillips, 2011) This project is a direct result of that funding.

Health and Safety

Safety was a major objective of the design and so has been addressed with toxicity analyses *in vitro*. The next step is to move into organismal models to ensure that the toxicity to specific tissues is not inhibitory to the use of UCNPs as a delivery vector for siRNA. As for any treatment, the health and safety of the patient is of utmost importance. The ultimate goal would be to target delivery of siRNA specifically to the motor neurons so that normal SOD1 in other tissues would not be affected. This would allow the treatment to specifically target a root cause of ALS, benefiting the most patients without negatively affecting the health of any other organ system. Whether or not this would lead to a restoration of motor function already lost by the patient remains to be seen. The goal is to stop progression.

Ethical Concern

The whole point of this project is to stop the progression of, or even reverse, the effects of a devastating degenerative disease. This would directly improve the lives of all patients receiving the treatment. Some ethical concerns that do come out of this are marketing, administration, and availability of the treatment. Marketing needs to be carefully monitored so that the expectations of patients do not exceed the limitations of the treatment. Patients need to be informed of exactly what the treatment does and when it is most effective or not effective at all so that they and their doctors can make an informed decision on whether to use this treatment. Administration of the treatment also has to be carefully constructed so as not to leave the patient in a worse condition. Any treatment targeting the central nervous tissue has to be carefully calibrated due to the sensitivity and importance of such structures. The next step of development for this system would use animal models to address this issue of administration. Since ALS is not a common

disease, cases are greatly dispersed across a global market. A viable treatment would need to be made available on multiple continents and would have to be accessible at varying socio-economic statuses. Therefore efforts must be made to keep production costs at a minimum while securing the proper approvals in multiple international markets.

Sustainability

The design of UCNPs has little effect on the environment. However, the manufacture of UCNPs on a large scale will require energy and material input. The manufacturing process can be made sustainable by drawing that energy and material from sustainable sources, such as solar power generators or low impact mining operations.

Manufacturability of UCNPs

As of now, UCNPs have only been used in very small quantities in a laboratory setting. Production of UCNPs has been tailored to meet the needs of this scale. Only small quantities of NPs are produced in 100-mL flasks (40-100 mg yield) at relatively low concentrations (0.1-10 mg/mL). If this is going to become a marketable treatment, production will have to meet the demands of a global market. Things to consider when manufacturing UCNPs on a large scale are scale of the production; cost of production, including initial materials and final yields; and difficulties of production, such as waste disposal and reaction conditions. First, the current process will be described and then broken down for manufacturability.

Currently, the manufacturing process of UCNPs is broken down into 4 steps, (1) assembly of the core/shell particle, (2) ligand exchange, (3) PEI conjugation, and (4) sterilization followed by centrifugation. The assembly of the core/shell particle is performed at high temperature (310^{O} C) in an inert atmosphere (argon gas) using an organic solvent (oleic acid). Since the shell of the particle is positively charged, the polar head of the oleic acid shields the particles from the nonpolar solvent. The core/shell are fully assembled but the linkage to oleic acid keeps the particle from being water-soluble. Toluene is used to scrub the particles from the oleic acid and transfer them into a partially polar environment (diethylene glycol). The solution is heated to 240 ^{O} C in the presence of citric acid. The toluene is boiled off and the oleic acid is replaced with citric acid making the particles water-soluble. The particles can then be suspended in an aqueous

solution of dimethyl sulfoxide and phosphate buffered saline at room temperature ($22\,^{O}C$). Aziridines are then added as precursors for branched polyethyleneimine (PEI). These link to the citric acid forming PEI-coated nanoparticles. The fully formed UCNPs are then sterilized by autoclave and then centrifuged to remove any excess PEI. This typically results in an 80% yield before centrifugation. (Production methods were drawn from the protocol developed by Shen, Jie of the Han Laboratory)

Cost of production is influenced by the initial cost of the material, the means of production, the amount produced per batch, and the final yield. The solvents and conjugates used are common and can be attained easily. The limiting material cost is the lanthanide metals used to form the core of the particle. However, recycling of the waste from the particle assembly and subsequent steps could lead to recovery of precursors and reduce overall costs. The means of production and the batch size are linked. Currently, the particles are produced in a laboratory using glassware assembled on-site. Increasing the batch size would require larger containers that can still maintain high temperatures and pressure. The most cost-effective solution would likely be batch reactors which are easily designed and maintained, widely used in industry and thereby readily available, and meet the specifications for temperature and pressure ranges associated with each step of the synthesis. Much like quantum dots, the industry demand for these particles would be on the one- to fifty-milligram scale per client. Therefore, the batch size would likely be less than five liters (minimally yielding two grams of UCNPs). Recycling the waste and using batch reactors to maintain reaction conditions would address the difficulties of production.

Chapter 7: Final Design and Validation

A need exists for an effective ALS therapy. Knockdown of mutated Superoxide Dismutase 1 has been proposed as a novel approach to disrupting the progression of ALS. Herein we proposed a design that utilizes RNAi to achieve this potentially therapeutic inhibition, however the delivery of siRNA presents challenges regarding safety, scalability, efficacy, and specificity. Thus, the specific objectives of this study were to assess the application of novel UCNPs as siRNA delivery vectors in these particular aspects. In order, their priority was determined to evaluate the success of the design:

1. Specificity
2. Scalability
3. Safety
4. Efficacy

It is important to note that while the achievement of each objective was evaluated directly by specific assays, objective priority did not determine the order in which the experiments were conducted. Instead, experiments were conducted in order of increasing complexity, as the results of simple experiments would guide the parameters chosen for the more complex procedures. Below, experiments are described in the chronological order in which they were performed, with the reasoning for choosing such order.

1. Safety was evaluated first because its measureable outcome had a design constraint; the cytotoxic effects of the particle dose could not compromise cell viability below 90%. As such, cytotoxicity assays were the first experiments conducted to ensure future experiments fell within tolerable particle dosages.

2. Following cytotoxicity assays, the binding ratios for plasmid and siRNA conjugation to NPs were derived. These assays provided specifications regarding the maximum payload saturation that could be delivered per NP. In effect, data from these tests enabled the team to scale the treatment to any desired quantity while maintaining maximum design efficiency.

3. The plasmid transfection experiment was performed next, to gauge the efficacy of the design. Specifically, measurable expression of GFP would indicate the efficacy of the delivery system compared to the control agent, lipofectamine.

4. In parallel with the plasmid transfection, siRNA transfections were performed to evaluate to final objective; specificity. The siRNA transfection provided samples with which Western blot analysis could be conducted. The analysis ultimately verified the specificity of treatment against the target protein, SOD1, as well as the efficacy of its silencing.

The cell line chosen to conduct these studies was the HeLa human cervical cancer line. Unless otherwise noted, all cultures were maintained and prepared using antibiotic-free, DMEM +10% FBS. All assays were performed in standard tissue culture polystyrene, and incubated at 37° C and 5% CO_2. All cell counts were determined by hemocytometer count without trypan blue exclusion staining.

Chapter 8: Conclusions and Recommendations

Conclusions

The experimental approach demonstrated several features regarding $NaYF_4$-shell UCNP activity in vitro. First, cytotoxicity assays characterized the workable range for $NaYF_4$-shell UCNP transfection, which was found to tolerate concentrations up to 20 µg/mL while maintaining 80% cell viability. This finding was followed by the demonstration of effective plasmid transfection quantified in correlation with GFP expression, which was 45% of the positive control, Lipofectamine™. Upon effective plasmid transfection, siRNA transfection verified payload protection through successful SOD1 knockdown. Relative to the PBS control, 45% knockdown was achieved.

CaF_2-shell UCNPs demonstrated a cytotoxicity profile with an improved range of tolerance compared to the $NaYF_4$ UCNPs. Cells were found to tolerate concentrations up to 50 µg/mL while maintaining 80% cell viability. While CaF_2-shell UCNPs could bind plasmid DNA, they did not demonstrate GFP expression upon transfection, suggesting insufficient intracellular payload release. Transfection with siRNA yielded similar results; although CaF_2-shell UCNPs were found to complex with siRNA at a 30:1 molar ratio (siRNA:UCNP), no significant ($p>0.05$) target knockdown was achieved.

Despite the shortcomings of the CaF_2-shell design, the $NaYF_4$-shell design demonstrated that UCNPs have potential as transfecting agents, in addition to their other valuable properties for imaging and tracking applications. Continued research and characterization with UCNPs could overcome the limitations in toxicity and transfection efficiency that are exhibited by the preliminary and final designs respectively.

The implication of SOD1 across all forms of ALS represents an opportunity for the application of RNAi –based therapy. Treatment with sequence specific siRNAs and UCNPs may target the cause of ALS, and if successful, could give rise to a model approach for treating other neurodegenerative disorders.

Recommendations

This study was limited in scope by time, UCNP availability, access to a single cell line, and small sample sizes. The following recommendations could be implemented in future studies to expand the current characterization of UCNPs for ALS therapy:

1. **Determine the cause for decreased transfection capacity in CaF_2-shell UCNPs.** Current data suggests that electrostatic payload-particle interactions are too strong to support delivery. Surface chemistry could be modified to allow for a similar binding ratio, with increased payload delivery.
2. **Repeat experiments in alternative cell lines**. ALS is a disease that affects the afferent motor neurons; ideally UCNPs should be tested in a neuronal cell line in vitro, to better characterize their efficacy prior to *in vivo* studies.
3. **Perform experiments with greater sample size.** To improve the consistency and accuracy of the data, the sample sizes should be increased. This is particularly pertinent regarding Western blotting, which can only be performed with 12 samples per blot.
4. **Utilize confocal microscopy to confirm endocytosis.** At this point it can only be assumed that successful GFP expression and SOD1 knockdown are the direct result of intracellular payload delivery by UCNPs. However, direct microscopic evidence would confirm UCNP endocytosis as the mechanism of delivery.
5. **Conduct ζ-potential and particle size measurements.** The ζ-potential is an indirect measure of surface charge and dispersion stability. Understanding how these properties affect UCNP functionality, could improve and guide the development of UCNPs for specific or alternative applications.
6. **Characterize the upconversion effect *in vitro*.** Confirm that UCNPs retain their upconverting properties after entering the cell. This could allow particle tracking to determine where the particles are being taken up (e.g., the spinal column and the corticospinal motor neurons).

Bibliography

Alshamsan, Aus, Haddadi, Azita, et al. (2009) “Formulation and delivery of siRNA by oleic acid and stearic acid modified polyethylenimine.” *Molecular Pharmaceuticals* **6**(1): 121-133. Web.

Bensimon, G., Lacomblez, L., & V. Meininger. (1994) "A Controlled Trial of Riluzole in Amyotrophic Lateral Sclerosis." *The New England Journal of Medicine* **330**(9): 585-591. Print.

Bosco, Daryl A., Brown Jr., Robert H., et al. (2010) “Wild-type and mutant SOD1 share an aberrant conformation and a common pathogenic pathway in ALS.” *Nature Neuroscience* **13**(11): 1396-1403. Web.

Clements, B.A., Incani, V. et al (2007) “A comparative evaluation of poly-l-lysine-palmitic acid and Lipofectamine ™ 2000 for plasmid delivery to bone marrow stromal cells”, *Biomaterials,* **28**(31): 4693-4704. Web.

Chen, Shao-Hua & Zhaori, Getu. (2010) “Potential clinical application of siRNA technique: benefits and limitations.” *European Journal of Clinical Investigation* **41**(2): 221-232. Web.

Congdon, Molly. (2010) *Synthesis of Near-IR Fluorophores Toward In Viv*o Protein Detection. (Unpublished Major Qualifying Project No. DEH MQP UMA3). Retrieved from Worcester Polytechnic Institute Electronic Projects Collection: http://www.wpi.edu/Pubs/E-project/Available/E-project-042910-162108/ p. 16. Web.

Duncan, R. (2003) “The Dawning Era of Polymer Therapeutics” *Nature Reviews Drug Discovery* **2**: 347-360. Web.

Epocrates Online. March 3, 2012. <https://online.epocrates.com/noFrame/showPage.do?method=drugs&MonographId=1196&ActiveSectionId=6>

Erbium Oxide; MSDS No. 25883 [Online]; Acros Organics N.V.: Fair Lawn, NJ, November 20, 2008, http://fscimage.fishersci.com/msds/25883.htm (accessed December 2, 2011).

Ferrari, M. (2009) “Cancer Nanotechnology: Opportunities and Challenges” *Nature Reviews Cancer* **5**: 161-171. Web.

Forsberg, K., Brännström, T., et al. (2010) “Novel Antibodies Reveal Inclusions Containing Non-Native SOD1 in Sporadic ALS Patients” *PLoS ONE* **5**(7): e11552. doi:10.1371/journal.pone.0011552. Web.

Grad, Leslie I., Cashman, Neil R., et al. (2011) “Intermolecular transmission of superoxide dismutase 1 misfolding in living cells” *Proceedings of the National Academy of Science* **108**(39): 16398-16403. Web.

Grimm, Dirk & Kay, Mark A. (2007) “Therapeutic application of RNAi: is mRNA targeting finally ready for prime time?” *Journal of Clinical Investigation.* **117** (12):3633-3641. Web.

Han, G., Wu, S., et al. (2009) “Non-blinking and photostable upconverted luminescence from single lanthanide-doped nanocrystals”. *Proceedings of the National Academy of Science* **106**(27): 10917-10921. Web.

IUPAC. (1997) Compendium of Chemical Terminology, 2nd ed. (the "Gold Book"). Compiled by A. D. McNaught and A. Wilkinson. Blackwell Scientific Publications, Oxford. XML on-line corrected version: http://goldbook.iupac.org (2006-) created by M. Nic, J. Jirat, B. Kosata; updates compiled by A. Jenkins. ISBN 0-9678550-9-8. doi:10.1351/goldbook. Web.

Jaiswal, Manoj, Kumar, et al. (2009) "Impairment of Mitochondrial Calcium Handling in a mtSOD1 Cell Culture Model of Motoneuron Disease." *BioMed Central Neuroscience* **10**(64): doi:10.1186/1471-2202-10-64. Web.

Lakowicz, J. R. (2006) In *Fluorophores;* Principles of Fluorescence Microscopy; Springer: 63-95. Print.

Luo, Dan & Saltzman, W. Mark. (2000) “Synthetic DNA Delivery Systems.” *Nature Biotechnology* **18**: 33-37. Web.

Massich, MD., Giljohann, DA. et al. (2009) “Regulating Immune Response Using Polyvalent Nucleic Acid−Gold Nanoparticle Conjugates” *Molecular Pharmaceutics* ***6***(6): 1934-1940. Web.

McQuarrie, D. A. & Simon, J. D. (1997) In *Lasers, Laser Spectroscopy and Photochemistry;* Physical Chemistry A Molecular Approach; University Science Books: Sausalito, California, 591-626. Print.

Miller, Timothy M., & Cleveland, Don W. (2005) "Treating Neurodegenerative Diseases with Antibiotics." *Science* **307**(5708): 361-362. Web.

Mitchell, J.D., & Borasio, G.D. (2007) "Amyotrophic Lateral Sclerosis." *The Lancet* **369**(9578): 2031-2041. Web.

National Institute of Neurological Disorders and Stroke. "ALS Fact Sheet." August 2, 2011 2011.Web. *NIH.* <http://www.ninds.nih.gov/disorders/amyotrophiclateralsclerosis/detail_ALS.htm>.

Paddison PJ. (2008) *RNA Interference*. Berlin: Springer, 2008. Print.

Pasinelli, Piera & Brown, Robert H. (2006)“Molecular biology of amyotrophic lateral sclerosis: insights from genetics.” *Nature Reviews: Neuroscience* **7**:710-723. Web.

Phillips, Frank. (2011) “Celucci to Take ALS Fight Public” Boston Globe [Boston] 19 May 2011, Metro: A.1+. Web.

Rosen, Daniel R., Brown, Robert H., et al. (1993) “Mutations in Cu/Zn superoxide dismutase gene are associated with familial amyotrophic lateral sclerosis” *Nature* **362**(6415): 59-62. Web.

Serda, R. E., Godin, B., Blanco, E., Chiappini, C., & Ferrari, M. (2011) “Multi-stage delivery nano-particle systems for therapeutic applications.” *Biochimica et Biophysica Acta* **1810**: 317-329. Web.

Shaw, PJ.,Chinnery, RM et al. (1997) “Immunocytochemical study of the distribution of the free radical scavenging enzymes CU/ZN superoxide dismutase (SOD1); MN superoxide dismutase (MN SOD) and catalase in the normal human spinal cord and in motor neuron disease” *Journal of Neurological Sciences* **147**: 115-125. Web.

Shi, Yang. (2003) “Mammalian RNAi for the masses” *Trends in Genetics* **19**(1): 9-12. Web

Thulium; MSDS No. D7120 [Online]; Mallinckrodt Baker: Phippsburg, NJ, May 25, 2005, http://www.jtbaker.com/msds/englishhtml/d7120.htm (accessed July 20, 2007).

Towne, Chris, Aebischer, Patrich, et al. (2011) “Neuroprotection by Gene Therapy Targeting Mutant SOD1 in Individual Pools of Motor Neurons Does Not Translate into Therapeutic Benefit in fALS Mice.” *Molecular Therapy* **19**(2): 274-283. Web.

Trotti, Davide et al. (1999) "SOD1 Mutants Linked to Amyotrophic Lateral Sclerosis Selectively Inactivate a Glial Glutamate Transporter." *Nature Neuroscience* **2**(9): 427-433. Web.

Wang, Y., Wong, J.F., et al. (2003) “‘Pulling’ Nanoparticles into Water: Phase Transfer of Oleic Acid Stabilized Monodisperse Nanoparticles into Aqueous Solutions of α-Cyclodextrin” *Nano Letters* **3**(11): 1555-1559. Web.

Wijesekera, Lokesh C. & Leigh, P. Nigel. (2009) "Amyotrophic Lateral Sclerosis." *Orphanet Journal of Rare Diseases* **4**(3): doi:10.1186/1750-1172-4-3. Web.

Worms, Paul M. (2001) "The Epidemiology of Motor Neuron Diseases: A Review of Recent Studies." *Journal of the Neurological Sciences* **191**(1-2): 3-9. Web.

Ytterbium Oxide; MSDS No. 96772 [Online]; Acros Organics N.V.: Fair Lawn, NJ, July 20, 2009, http://www.jtbaker.com/msds/englishhtml/d7120.htm (accessed December 2, 2011).

Glossary

ALS – Amyotrophic Lateral Sclerosis

DMEM – Delbucco's Modified Eagle Medium

EtBr – Ethidium Bromide

fALS – Familial ALS

FBS – Fetal Bovine Serum

GFP – Green fluorescent protein

HRP – Horseradish Peroxidase

NIH – National Institute of Health

NINDS – National Institute of Neurological Disorders and Stroke

NP – Nanoparticle

PBS – Phosphate Buffered Saline

PCC – Pairwise Comparison Chart

PEI – Polyethylene Imine

RNAi – RNA interference

sALS – Sporadic ALS

siRNA – small interfering RNA

SOD1 – Superoxide Dismutase 1

UCNP – Upconverting Nanoparticle

Appendix A: Objectives

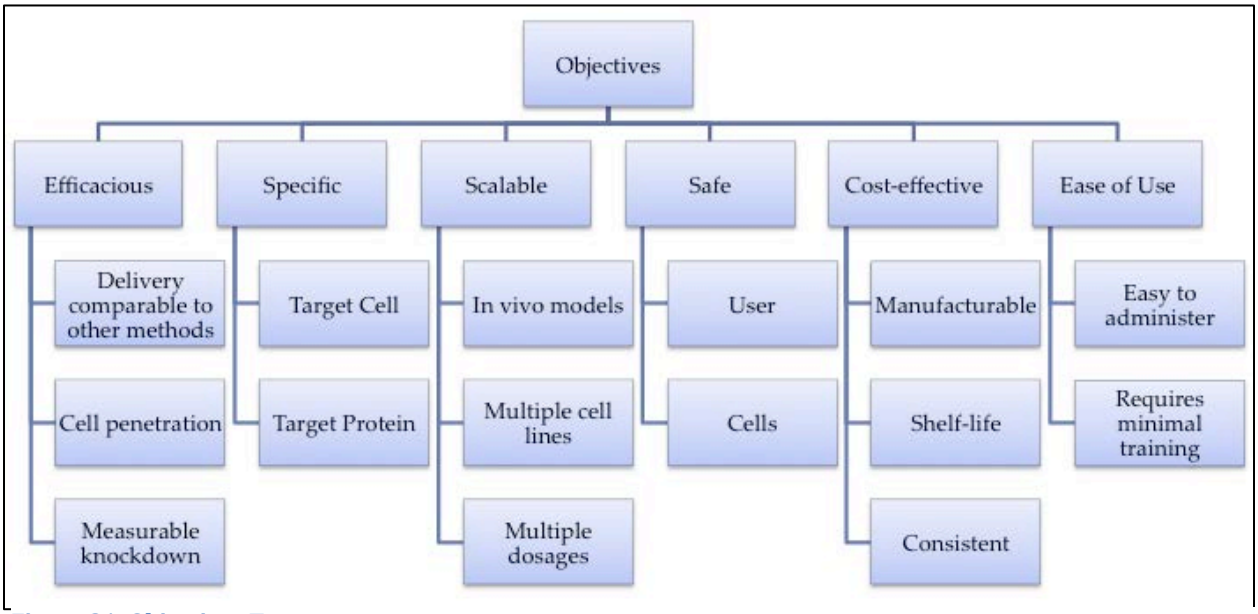

Figure 21: Objectives Tree

The objectives tree organizes the primary and secondary objectives of the final design. In the first row the primary objectives are arranged. Below each primary objective, secondary sub-objectives follow. For example; for the primary objective of Safety, the sub-objectives detail that the design be safe for the user delivering the therapy and the cells receiving the therapy.

Table 2: PCC for Efficacy Sub-objectives

	Comparable	Penetration	Knockdown	Total
Comparable	—	0	0	0
Penetration	1	—	0	1
Knockdown	1	1	—	2

To measure efficacy, the extent of protein knockdown is of highest priority. Second is the ability of the therapy to penetrate the cell, and of least priority is the efficacy in comparison to other delivery methods.

Table 3: PCC for Sub-Objective – Scalable

	In Vivo	Cell Lines	Dosages	Total
In Vivo	—	1	1	2
Cell Lines	0	—	1	1
Dosages	0	0	—	0

The highest priority for scalability is that the design be scalable to in vivo models. Next, the design should be scalable to multiple cell lines, and least importantly to multiple doses.

Table 4: PCC for Sub-Objective- Specific

	Cell	Protein	Total
Cell	—	0	0
Protein	1	—	1

Specificity to target the protein is of higher priority than to target the cell.

Table 5: PCC for Sub-Objective – Safe

	User	Cells	Total
User	—	1	1
Cells	0	—	0

The safety of the user is of higher priority than the safety of the cells receiving the therapy.

Appendix B: Lab Protocols

GFP Plasmid Transfection

SJK 8/5/2011
Han Laboratory

Protocol: GFP Plasmid Transfection with Core/Shell Nanoparticles in HeLa Cells

1. **Seeding**

   For 96 well plate:
   Seed 96-well black plate at **7,500 cells/well** and incubate overnight in 5% CO2 incubator. After calculating cell density, add **DMEM + 10%FBS** to cell suspension so to achieve a **total loading volume of 90 uL/well.** *Note: media is antibiotic-free.*

   For 6-well plate:
   Seed at **250,000 cells/well** and incubate overnight in 5% CO2 incubator. After calculating cell density, add **DMEM + 10%FBS** to cell suspension so to achieve a **total loading volume of 3mL/well.** *Note: media is antibiotic-free.*

2. **Transfection**

   ***Before loading, aspirate all media and replace with low-serum Opti-MEM media.**

   Nanoparticle-DNA complexes: Conjugate nanopaticles with plasmid for each desired concentration parameter. Add nanoparticles and DNA, then PBS so to achieve a final loading volume of **25 uL/well (96-well) or 0.83mL/well (6-well)**. Allow 5 minutes for NP-DNA-PBS cocktail to complex prior to loading. Agitate with pipette prior to loading.

   Allow 4 hours incubation time after loading**, then aspirate wells and replace with DMEM+10% FBS.** Read plate absorbance at 24 and 48 hours post-transfection.

Western Blotting for siRNA Transfection

Han Laboratory
Procedure for Western Blotting
SJK 8/5/11

1. **Sample Harvest**

    a. Wash Cells 3X with PBS buffer to remove phenol red from culture
    b. Add 200 uL per well (for 12 well plate) of M-PER buffer + P.I.
    c. Shake/agitate for 5 minutes
    d. Collect lysate, centrifuge at 14,000 x g for 5 minutes
    e. Transfer supernatant to new sample tube
    f. Freeze in -20° C

2. **Perform BCA Assay (Microplate Procedure)**

    a. Denature protein in samples with hot water bath at 95° C for 5 minutes (Only denature what you need! Do not denature entire sample and refreeze. Denture enough for BCA and Western; 35 to 50 uL each)
    b. Vortex samples and pipette 25 uL of each sample or standard into microplate well (10uL may be used but working range become limited to 125-2000ug/mL)
    c. Add 200 uL of working reagent to each well (WR prepared 50A:1B)
    d. Shake gently for 30 seconds
    e. Incubate at 37° C for 30 minutes
    f. Cool Plate to RT
    g. Measure absorbance at 562 nm

3. **Gel Loading**

    a. Prepare samples with equivalent protein quantity. If necessary, dilute with M-PER buffer + P.I. (Loading volume = 30 uL; 24 sample + 6 lammelli blue dye)
    b. Prepare fresh Tris-Glycine-SDS Running Buffer (about 1.5 – 2 L needed)
    c. Insert gel into blotting box; remove plastic strip on pre-cast gels and face gel inward to box (the high side of the plastic casing should face outward)
    d. Fill box with running buffer, above the top of the gel. Ensure no bubbles are above the loading wells.
    e. Load samples + Ladder (Precision Plus "Dual Color" ladder requires 10uL)
    f. Run Gel at 70 V for 120 minutes.

4. Transfer

a. Prepare transfer buffer solution with 10% MeOH; Soak sponges, Whattman paper, and nitrocellulose membrane
   Carefully remove gel from casing, load in order onto clamping apparatus: Clamp, Sponge, Paper, Gel, Membrane, Paper, Sponge, Clamp. Roll tube across paper to ensure no bubbles are trapped between the gel and membrane.
b. Insert clamp into transfer box. Ensure the side of the gel adjacent to the membrane faces the positive (Red) face of the box, or samples will transfer out of the blot and be lost in solution.
c. Run at 100 V for 1 hour

5. Blocking, Add Antibodies

d. Cut membrane between proteins of interest. (α-Tubulin ~50 kDa, SOD1 ~20 kDa)
e. Rinse membrane in PBST 3 x 5 min
f. Block membrane in PBST + 5% milk for 1 h RT
g. Replace with 10 mL new PBST + 5% milk and add 1° antibody:
   i. 1° dilution α-Tubulin – 1: 5000 (2 uL)
   ii. 1° dilution SOD1 – 1:10,000 (1 uL)
h. Incubate overnight on shaker at 4°C
i. Wash membrane 3 x 5 min with PBST
j. Add 2° antibody in 10 ml PBST + 5% milk
   i. 2° dilution α-Tubulin – 1: 10,000 (1 uL)
   ii. 2° dilution SOD1 – 1:2000 (5 uL)
k. Incubate on shaker 1 hr RT
l. Wash 3 x 5 min in PBST

6. Chemiluminescence and Imaging

m. At 4°C, prepare chemiluminescent solution (SuperSignal West Pico) at 1:1 volumetric ratio. 4 mL per membrane is sufficient. Work Fast!
n. Pipette solution into membrane boxes; let shake 5 min
o. Place membranes into plastic film for imaging; roll any bubbles out of film
p. Image on LAS 4000 using chemiluminescence setting. Exposure increment = 10 s. Adjust brightness/contrast as necessary.